AGU PUBLICATIONS

Paleoceanography

RESEARCH ARTICLE
10.1002/2016PA002985

Key Points:
- Sediments from the U.S. mid-Atlantic margin capture thick shelf records of the PETM
- Foraminiferal isotopic records from NJ cores show different responses in surface versus deep taxa
- Isotopic trends are interpreted to reflect changes in bloom season and/or in shelf hydrography

Supporting Information:
- Supporting Information S1
- Figure S1
- Figure S2
- Figure S3

Correspondence to:
M. Makarova,
maria.makarova@rutgers.edu

Citation:
Makarova, M., J. D. Wright, K. G. Miller, T. L. Babila, Y. Rosenthal, and J. I. Park (2017), Hydrographic and ecologic implications of foraminiferal stable isotopic response across the U.S. mid-Atlantic continental shelf during the Paleocene-Eocene Thermal Maximum, *Paleoceanography*, *32*, doi:10.1002/2016PA002985.

Received 1 JUN 2016
Accepted 21 DEC 2016
Accepted article online 29 DEC 2016

Hydrographic and ecologic implications of foraminiferal stable isotopic response across the U.S. mid-Atlantic continental shelf during the Paleocene-Eocene Thermal Maximum

Maria Makarova[1], James D. Wright[1,2], Kenneth G. Miller[1,2], Tali L. Babila[3,4], Yair Rosenthal[1,2,3], and Jill I. Park[1]

[1]Department of Earth and Planetary Sciences and Institute of Earth, Oceans, and Atmospheric Sciences, Rutgers, The State University of New Jersey, Piscataway, New Jersey, USA, [2]Institute of Earth, Ocean, and Atmospheric Sciences, Rutgers, The State University of New Jersey, New Brunswick, New Jersey, USA, [3]Department of Marine and Coastal Sciences, Rutgers, The State University of New Jersey, New Brunswick, New Jersey, USA, [4]Department of Earth and Planetary Sciences, University of California, Santa Cruz, California, USA

Abstract We present new $\delta^{13}C$ and $\delta^{18}O$ records of surface (*Morozovella* and *Acarinina*) and thermocline dwelling (*Subbotina*) planktonic foraminifera and benthic foraminifera (*Gavelinella*, *Cibicidoides*, and *Anomalinoides*) during the Paleocene-Eocene Thermal Maximum (PETM) from Millville, New Jersey, and compare them with three other sites located along a paleoshelf transect from the U.S. mid-Atlantic coastal plain. Our analyses show different isotopic responses during the PETM in surface versus thermocline and benthic species. Whereas all taxa record a 3.6–4.0‰ $\delta^{13}C$ decrease associated with the carbon isotope excursion, thermocline dwellers and benthic foraminifera show larger $\delta^{18}O$ decreases compared to surface dwellers. We consider two scenarios that can explain the observed isotopic records: (1) a change in the water column structure and (2) a change in habitat or calcification season of the surface dwellers due to environmental stress (e.g., warming, ocean acidification, surface freshening, and/or eutrophication). In the first scenario, persistent warming during the PETM would have propagated heat into deeper layers and created a more homogenous water column with a thicker warm mixed layer and deeper, more gradual thermocline. We attribute the hydrographic change to decreased meridional thermal gradients, consistent with models that predict polar amplification. The second scenario assumes that environmental change was greater in the mixed layer forcing surface dwellers to descend into thermocline waters as a refuge or restrict their calcification to the colder seasons. Although both scenarios are plausible, similar $\delta^{13}C$ responses recorded in surface, thermocline, and benthic foraminifera challenge mixed layer taxa migration.

1. Introduction

The Paleocene-Eocene Thermal Maximum (PETM) was an abrupt warming event initiated at the beginning of the Eocene (~56 Ma) and characterized by a global temperature increase of about 4–8°C [*Kennett and Stott*, 1991; *Bralower et al.*, 1995; *Thomas et al.*, 1999; *Zachos et al.*, 2003; *Tripati and Elderfield*, 2004; *Sluijs et al.*, 2006; *Dunkley Jones et al.*, 2013]. The PETM is associated with the carbon isotope excursion (CIE) represented by a decrease in $\delta^{13}C$ values in marine (~2–3‰ in benthic and ~2.5–4‰ in planktonic foraminifera) [*Kennett and Stott*, 1991; *Zachos et al.*, 2007; *McInerney and Wing*, 2011] and terrestrial (~2.5–7‰) [*Koch et al.*, 1992; *Wing et al.*, 2005; *McInerney and Wing*, 2011; *Bowen et al.*, 2015] environments requiring a substantial addition of light carbon (^{12}C) into global reservoirs. The CIE can be subdivided into four stages: (1) the initiation of the $\delta^{13}C$ decrease termed the CIE onset [*Röhl et al.*, 2007] that was used to correlate the Paleocene/Eocene (P/E) boundary stratotype at Dababiya, Egypt [*Aubry et al.*, 2007]; (2) a sharp $\delta^{13}C$ decrease, the rapidity of which is contentious [cf., *Cui et al.*, 2011; *Wright and Schaller*, 2013], although most studies estimate that the decrease occurred in several thousand years or less [e.g., *Kennett and Stott*, 1991; *Bowen et al.*, 2015; *Kirtland Turner and Ridgwell*, 2016; *Zeebe et al.*, 2016]; (3) a period of stable low carbon isotope values, termed the CIE "core" [*Röhl et al.*, 2007; *Stassen et al.*, 2012], the duration of which is uncertain, with astronomical estimates on the order of 40 kyr [*Katz et al.*, 1999] to 80 kyr [*Röhl et al.*, 2007] and ^{3}He-based chronology of ~135 kyr [*Murphy et al.*, 2010]; and (4) an exponential recovery period to near pre-CIE values of ~80 kyr [*Murphy et al.*, 2010] to ~120–140 kyr [*Dickens et al.*, 1997; *Katz et al.*, 1999; *Röhl*

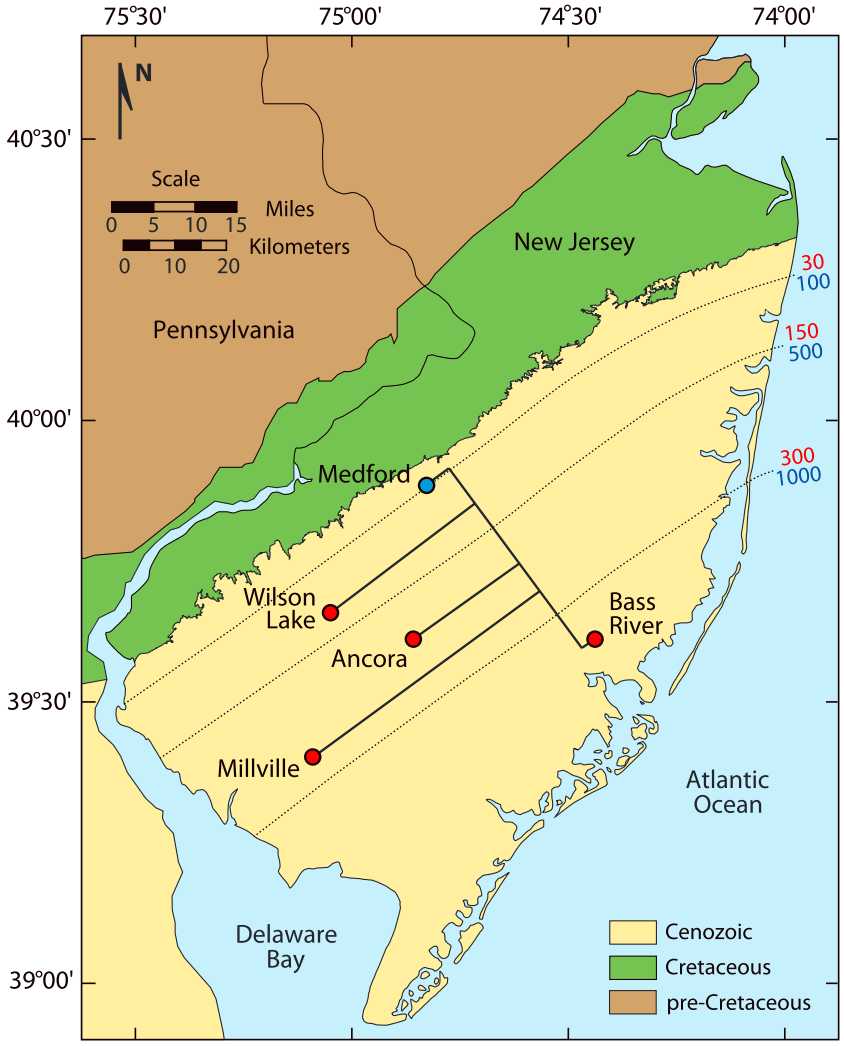

Figure 1. Location map of the PETM sections on the New Jersey coastal plain: Wilson Lake, Ancora, Millville, and Bass River. Red circles indicate the New Jersey coreholes, and blue circle shows an anchor point at Medford, NJ, used for paleodepth reconstructions during Vincentown deposition. Black solid lines represent the projection of sites onto a dip profile drawn through Medford outcrop and Bass River. Dashed lines indicate the structural contours from *Zapecza* [1984] with depths to the top of the Campanian in meters (red) and feet (blue) (modified after *Esmeray-Senlet et al.* [2015]).

et al., 2007]. The majority of PETM foraminiferal isotope records are from open ocean cores that have thinner, lower-resolution CIE "core" intervals of ~1 m or less [e.g., *Kennett and Stott*, 1991; *Bralower et al.*, 1995; *Thomas et al.*, 1999; *Thomas et al.*, 2002; *Zachos et al.*, 2003; *Hollis et al.*, 2015]. The CIE onset and "core" in deep-sea records are generally truncated owing to the corrosive conditions in bottom waters at the onset of the PETM and therefore dissolution of calcium carbonate sediments on the seafloor [*Zachos et al.*, 2005; *Bralower et al.*, 2014].

Stratigraphically more complete in regard to the CIE onset and "core" and much thicker (up to ~11 m) marine PETM sections are found along the New Jersey paleoshelf (Figures 1 and 2) [*Cramer et al.*, 1999; *Zachos et al.*, 2006; *John et al.*, 2008; *Harris et al.*, 2010; *Wright and Schaller*, 2013]. An advantage of the New Jersey paleoshelf is its location on a passive margin with relatively simple tectonics that allows paleodepth reconstructions and higher temporal resolution due to high sedimentation rates (>10 m deposited during the core, requiring rates >20 cm/kyr using astronomical time scales). The P/E boundary in New Jersey is accompanied by a lithologic change from sandy silts of the underlying Vincentown Formation to clayey silts of the overlying Marlboro Formation (Figure 3) [*Gibson et al.*, 1993; *Cramer et al.*, 1999; *Sugarman et al.*, 2005; *Kopp et al.*, 2009; *Lombardi*, 2013]. The clayey-silt-rich lithology of the Marlboro Formation acts as an

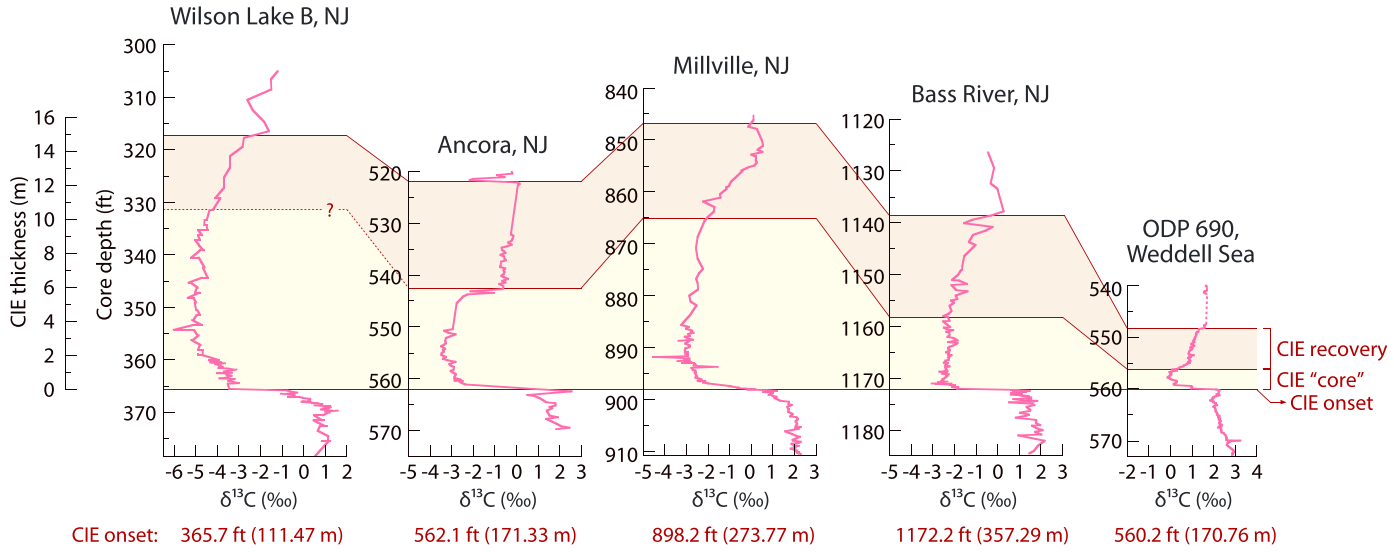

Figure 2. Correlation of bulk carbonate $\delta^{13}C$ records between the New Jersey coastal plain ODP sites Wilson Lake Hole B [*Wright and Schaller*, 2013]; Ancora [this study]; Millville [this study]; Bass River [*Cramer et al.*, 1999; *John et al.*, 2008]; and open ocean ODP Site 690, the Weddell Sea [*Bains et al.*, 1999]. Records are aligned on the CIE onset and correlated at the CIE "core" and recovery sections. Vertical scale is uniform to demonstrate different resolution of the CIE "core" and recovery intervals among the sites.

impermeable barrier to fluid interaction with carbonate sediments providing excellent preservation of foraminifera as seen in other clay-rich marine sections [e.g., *Pearson et al.*, 2001; *Sexton et al.*, 2006]. Planktonic foraminifera from the underlying sandier Vincentown Formation are less well preserved [*Zachos et al.*, 2006; *Babila et al.*, 2016].

The aim of this study is to understand the spatial and temporal hydrographic responses on the continental shelf to climate change during the PETM. The hydrography along shelf is dynamic as physical processes are governed by the interplay between land and open ocean interactions, including storms, coastal currents, and freshwater inputs [*Gong et al.*, 2010]. An approach to resolve regional from global isotopic marine trends is to construct a cross-shelf transect with sites that range in coastal proximity and environmental influence. Here we sampled the PETM in a shelf transection of four cores drilled as part of the New Jersey Ocean Drilling Program (ODP) Leg 174AX: Wilson Lake (Holes A and B), Ancora, Millville, and Bass River, with Wilson Lake being the most nearshore and Bass River being the furthest offshore (Figure 1) [*Miller et al.*, 1998; *Miller et al.*, 1999; *Sugarman et al.*, 2005].

Stable isotope studies of planktonic (surface and deep dwelling) and benthic foraminifera from expanded shelf records provide insights into hydrographic changes in the mixed layer versus thermocline and deeper layers during the PETM. Although previous studies have provided evidence for an enhanced hydrological cycle on the U.S. mid-Atlantic shelf [e.g., *Kopp et al.*, 2009; *Stassen et al.*, 2012, 2015], we currently lack a comprehensive reconstruction of cross-shelf hydrography. Here we present new stable isotope ($\delta^{13}C$ and $\delta^{18}O$) records of multiple taxa from Millville, combining them with previously published data from Wilson Lake, Ancora, and Bass River [*Cramer et al.*, 1999; *Cramer and Kent*, 2005; *Zachos et al.*, 2006; *Zachos et al.*, 2007; *John et al.*, 2008; *Stassen et al.*, 2012; *Babila*, 2014; *Babila et al.*, 2016]. We analyzed surface mixed layer dwelling foraminiferal species in two genera (*Morozovella* and *Acarinina*); thermocline dwelling foraminiferal species of the genus *Subbotina*; and benthic foraminiferal species of *Cibicidoides*, *Anomalinoides*, and *Gavelinella*. We employ the fact that planktonic foraminifera occupy different habitats to reconstruct $\delta^{13}C$ and $\delta^{18}O$ depth profiles [e.g., *Fairbanks et al.*, 1982; *Boersma et al.*, 1987; *Pearson et al.*, 1993; *Bralower et al.*, 1995; *Lu and Keller*, 1996; *Coxall et al.*, 2000; *Pearson et al.*, 2001]. We compile vertical isotope profiles from New Jersey cores to reconstruct the water column structure along the continental shelf. The strength of our reconstructions is the spatial coverage afforded by a cross-shelf transect and temporal resolution allowed by relatively high sedimentation rates on the New Jersey paleoshelf minimizing the effects of bioturbation.

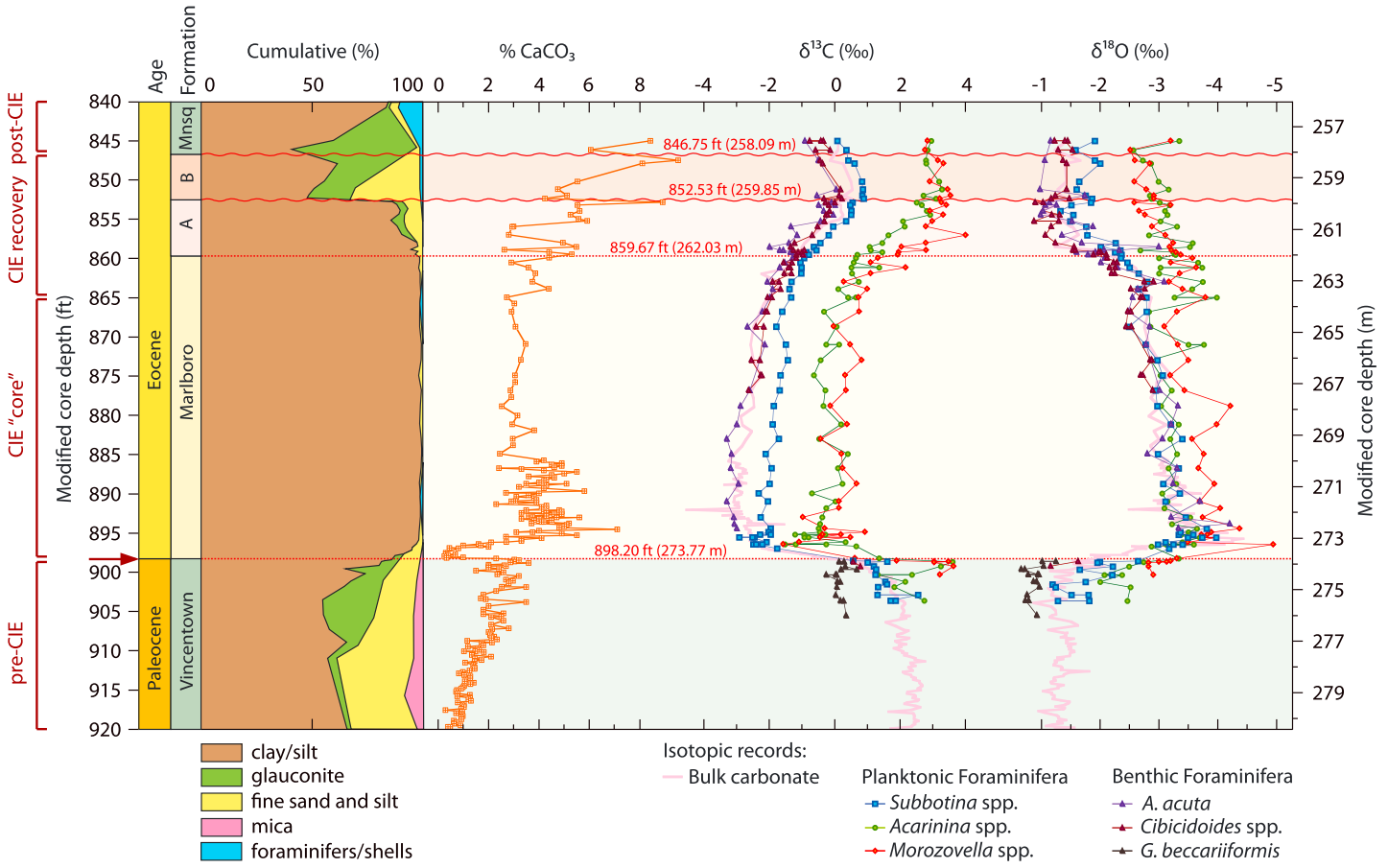

Figure 3. Compilation of records at Millville, NJ: cumulative grain size, % $CaCO_3$, $\delta^{13}C$, and $\delta^{18}O$ (plotted in reverse order) of bulk carbonate, planktonic, and benthic foraminifera. Bulk carbonate data are from this study and *Wright and Schaller* [2013]. Thermocline dwellers *Subbotina* spp. are in blue and surface dwellers *Morozovella* spp. and *Acarinina* spp. are in red and green, respectively. For benthic foraminifera, *Gavelinella beccariiformis* is shown in black, *Anomalinoides acuta* in purple, and *Cibicidoides* spp. in brown. Wavy red lines represent the sharp unconformable contacts, and dashed red lines indicate the gradational contacts between the formations. Arrow indicates the CIE onset. Depths are modified and corrected for core expansion. Both corrected and modified core depths are given in Table S1. Mnsq = Manasquan Formation.

2. ODP Leg 174AX Millville Site

ODP Leg 174AX Millville core recovered the Vincentown, Marlboro, and Manasquan Formations (257.55–280.33 m) that span the Paleocene/Eocene boundary (Figure 3). The Vincentown Formation is a micaceous, glauconitic, sandy silt at Millville. The contact between the Vincentown and Marlboro Formations occurs within a 0.6 ft transition zone with decreasing upward glauconite and coarse fraction content. Clayey silts (mean grain size 8 μm) of the Marlboro Formation comprise an expanded CIE "core" (10 m thick) at Millville. The CIE recovery interval (5.5 m thick) captures a lithologic transition from the Marlboro Formation to coarser informal units referred to as A and B here (discussed in the supporting information). The post-CIE section consists of glauconitic, carbonate-rich sandy silts of the Manasquan Formation overlying unit B above an unconformity at 258.09 m. For more information on lithostratigraphy and paleowater depth estimates, see the supporting information.

The Millville site provides advantages over other New Jersey coastal plain sites. It has higher sedimentation rates and temporal resolution than further offshore Bass River, but it is still deep enough to sample the water column from the mixed layer to thermocline and colder bottom waters that is missing in the upper Paleocene sections of the updip Ancora and Wilson Lake cores. Deposition at Millville was below storm wave base in the middle neritic zone allowing reconstruction of the full range of foraminiferal isotopic gradients distributed throughout the water column. The Millville core recovered sufficient well-preserved pre-CIE foraminifera (273.77–275.40 m) used to establish isotopic changes across the CIE onset, although there is a thin low

carbonate interval (<1%; 273.38–273.77 m) above the CIE onset [this study; *Wright and Schaller*, 2013] with no foraminifera (Figure 3). The sharp $\delta^{13}C$ decrease at Millville appears within the Vincentown/Marlboro transitional interval at 273.77–273.95 m. In comparison, the updip Wilson Lake and Ancora cores also record gradational lithologic transitions into the PETM, but resolution of the isotopic records is limited because there are insufficient planktonic foraminifera for a full suite of geochemical analyses within the upper Paleocene [*Zachos et al*., 2006; *Babila*, 2014]. Conversely, the uppermost Paleocene section at the deepest water Bass River core recovered the highest foraminiferal abundances [*Zachos et al*., 2007; *John et al*., 2008; *Babila et al*., 2016]; however, the CIE initiation at Bass River appears to be truncated [*John et al*., 2008; *Stassen et al*., 2012], possibly yielding incomplete records. Thus, Millville is located in the ideal setting to contain more continuous lithologic and foraminifera-rich marine sediment archive to generate detailed stable isotope records of the PETM from shelf.

3. Methods

3.1. Analyses

Core samples were disaggregated in a sodium metaphosphate solution (5.5 g of sodium metaphosphate per liter) to deflocculate clays and then washed through a 63 μm sieve to remove the fine fraction (<63 μm). The >63 μm fraction was dried overnight in a 50°C oven and weighed dry to compute the percentage of coarse sediment. Subsamples for percent calcium carbonate (% $CaCO_3$) and stable isotope ($\delta^{13}C$ and $\delta^{18}O$) measurements of bulk sediment were dried overnight in a 50°C oven and homogenized using a mortar and pestle.

For stable isotope analysis of planktonic foraminifera, specimens of *Morozovella* (*M. aequa*, *M. acuta*, *M. subbotinae*, and *M. velascoensis*), *Acarinina* (*A. soldadoensis*, *A. esnehensis*, *A. coalingensis*, and *A. angulosa*), and *Subbotina* (*S. roesnaesensis*, *S. velascoensis*, *S. triangularis*, and *S. hornibrooki*) were picked mainly from the >250 μm size fraction using the taxonomy of *Olsson et al*. [1999] and *Pearson et al*. [2006]. For stable isotope analysis of benthic foraminifera, specimens of *Gavelinella beccariiformis*, *Anomalinoides acuta*, and *Cibicidoides* (*C. alleni*, *C. howelli*, and *C. succedens*) were picked mainly from the >250 μm size fraction using the taxonomy of *Cushman* [1951] and *Berggren and Aubert* [1975]. To avoid species bias, most of the samples analyzed consisted of single species of one size fraction (Data Set S1 in the supporting information). However, uneven distribution of single species throughout the section precluded compilation of continuous monospecific records compelling us to present the data by genera. Comparison of monospecific multispecimen analyses at Millville (Data Set S1 and Figure S1 in the supporting information) and elsewhere [e.g., *Pearson et al*., 1993; *Bralower et al*., 1995; *Babila et al*., 2016] justifies compilation of monogeneric records.

Stable isotope analyses of foraminifera and bulk sediment were conducted on a Micromass Optima mass spectrometer with an attached multiprep device. Carbonate samples were reacted in 100% phosphoric acid (H_3PO_4) at 90°C for 15 min, and the evolved CO_2 gas was collected in a liquid nitrogen cold finger. Ratios are reported in standard delta notation in parts per thousand (per mil, ‰) $\delta = [(R_{sample}/R_{standard}) - 1] \times 1000$, where $R = {}^{13}C/{}^{12}C$ or ${}^{18}O/{}^{16}O$, relative to Vienna Pee Dee belemnite ($\delta^{13}C_{VPDB}$ and $\delta^{18}O_{VPDB}$). One-sigma analytical errors based on analyses of an internal laboratory reference material (~8 standards for every 24 samples) are ±0.05‰ and ±0.08‰ for $\delta^{13}C$ and $\delta^{18}O$, respectively.

Percent carbonate values were determined by converting the transducer reading for each sample analysis to a mass of $CaCO_3$ using an empirically derived calibration based on sample weight and transducer readings.

Depths of lithologic boundaries and samples at Millville reported here are modified for core expansion by adjusting the core recovery length to a 10 ft (~3 m) interval per run [*Sugarman et al*., 2005]. The true core depths of analyzed samples are given in Data Set S1.

3.2. Correction for Test Size

Most of the samples analyzed from the section below the CIE onset were picked from a smaller size fraction of 150–200 μm due to the lack of larger specimens in this interval. We applied a $\delta^{13}C$ correction for test size to allow comparison of carbon isotopic values from the pre-CIE samples that contain smaller specimens to the rest of the Millville section. *Morozovella* and *Acarinina* are considered obligate symbiont-bearing surface dwellers with well-established positive $\delta^{13}C$ to test size correlation [e.g., *Pearson et al*., 1993; *D'Hondt et al*., 1994; *Norris*, 1996; *Quillévéré et al*., 2001]. We applied a 1‰ correction in $\delta^{13}C$ per 100 μm test size change

that was previously quantified for *Morozovella* and *Acarinina* [e.g., *Norris*, 1996; *Tripati and Elderfield*, 2004; *Wade et al*., 2008; *Birch et al*., 2012]. Asymbiotic thermocline dwelling *Subbotina* also exhibit a test size-dependent $\delta^{13}C$ offset; however, this effect is likely due to increased kinetic fractionation observed in almost all foraminifera $<150\,\mu m$ [*D'Hondt and Zachos*, 1993; *Bornemann and Norris*, 2007; *Birch et al*., 2012]. We measured $\delta^{13}C$ in *Subbotina roesnaesensis* from small (150–212 μm) and large (250–300 μm) size fractions at Wilson Lake Hole B and detected a consistent offset of $0.41 \pm 0.05‰$ ($n = 4$) between small and large specimens (Table S2 in the supporting information). *Bornemann and Norris* [2007] showed a similar change of 0.3–0.5‰ in $\delta^{13}C$ per test size due to higher metabolic activity in smaller foraminifera. Accordingly, we applied a 0.4‰ correction in $\delta^{13}C$ for small (150–212 μm size fraction) specimens of *Subbotina* at Millville. Measured and corrected for test size $\delta^{13}C$ values in all analyzed planktonic foraminifera are given at Data Set S1. These corrections only apply to $\delta^{13}C$ data because previous studies of test size effects on oxygen isotopic values indicated no consistent change in $\delta^{18}O$ with foraminiferal test size variation [e.g., *Norris*, 1996; *Wade et al*., 2008; *Birch et al*., 2012]. Similarly, benthic foraminiferal vital effects can be minimized by measurements of monospecific samples from the larger size fraction [*Katz et al*., 2010].

3.3. Planktonic Foraminiferal Depth Habitats

We used $\delta^{18}O$ as a relative indicator of ocean temperature to estimate a depth ranking of planktonic foraminifera, subdividing them into surface (mixed layer) and deep (thermocline) dwellers. The $\delta^{18}O_{calcite}$ is controlled in part by the temperature of the surrounding seawater from which the foraminiferal test is precipitated [*Epstein et al*., 1953] and thus is used to constrain the temperature of habitats occupied by extinct planktonic foraminifera [e.g., *Emiliani*, 1954; *Boersma et al*., 1987; *Pearson et al*., 1993, 2001; *Coxall et al*., 2000]. Most studies assume that the stable isotopic differences reflect calcification at different depths. Accordingly, high $\delta^{18}O$ values of *Subbotina* spp. reflect calcification in colder thermocline waters, whereas lower $\delta^{18}O$ values of *Morozovella* spp. and *Acarinina* spp. indicate warmer temperatures in the surface mixed layer. Moreover, measurements of $\delta^{11}B$ in foraminiferal tests that reflect seawater pH also support this depth habitat ranking [*Pearson and Palmer*, 1999; *Anagnostou et al*., 2016]. However, generic differences in $\delta^{18}O$ values could reflect seasonal differences, as they do in modern assemblages [e.g., *Bé*, 1960; *Curry et al*., 1983; *Thunell et al*., 1983; *Deuser and Ross*, 1989; *Ravelo and Fairbanks*, 1992]. In the middle to high latitudes, seasonal variability in light and other environmental properties control the "blooms" of different species, and these seasonal variations in surface temperature and nutrients can mimic mean annual vertical conditions. Since vertical temperature gradients that develop in the spring and summer to a large part reflect the seasonal temperature changes in surface water, we discuss isotopic gradients between them as surface to thermocline differences.

Morozovella spp. and *Acarinina* spp. record higher $\delta^{13}C$ values relative to *Subbotina* spp. mirroring typical vertical nutrient profiles [e.g., *Boersma et al*., 1987; *Pearson et al*., 1993; *Bralower et al*., 1995; *Lu and Keller*, 1996; *Coxall et al*., 2000]. Near-complete removal of nutrients by biological productivity increases dissolved inorganic carbon $\delta^{13}C$ values in the surface mixed layer. Organic matter remineralization occurs within the seasonal thermocline on the continental shelf in the lower photic zone (25–50 m) [*Fairbanks and Wiebe*, 1980; *Glenn et al*., 2008]. The net effect results in higher $\delta^{13}C$ values in *Morozovella* spp. and *Acarinina* spp. and lower $\delta^{13}C$ values of *Subbotina* spp. We note that seasonal blooms would produce similar stable isotope patterns as described versus depth. Such isotopic relationships between *Morozovella*, *Acarinina*, and *Subbotina* are also reported from PETM sections at New Jersey coastal plain sites Wilson Lake Hole A, Ancora, and Bass River [*Zachos et al*., 2006, 2007; *John et al*., 2008; *Babila*, 2014; *Babila et al*., 2016], as well as from open ocean sites [e.g., *Kennett and Stott*, 1991; *Bralower et al*., 1995; *Lu and Keller*, 1996; *Thomas et al*., 2002; *Tripati and Elderfield*, 2004; *Hollis et al*., 2015].

4. Results

4.1. Millville Foraminiferal Isotopic Records

We recognize the CIE onset at Millville by a sharp decrease in bulk $\delta^{13}C$ values and by a drop in percent carbonate at 273.77 m (Figures 2 and 3), delineated in detailed bulk $\delta^{13}C$ records by *Wright and Schaller* [2013]. This decrease is recognized not only by its large amplitude but also by biostratigraphic data that clearly put it at the P/E boundary [*Sugarman et al*., 2005]. Using the bulk $\delta^{13}C$ record [this study and *Wright*

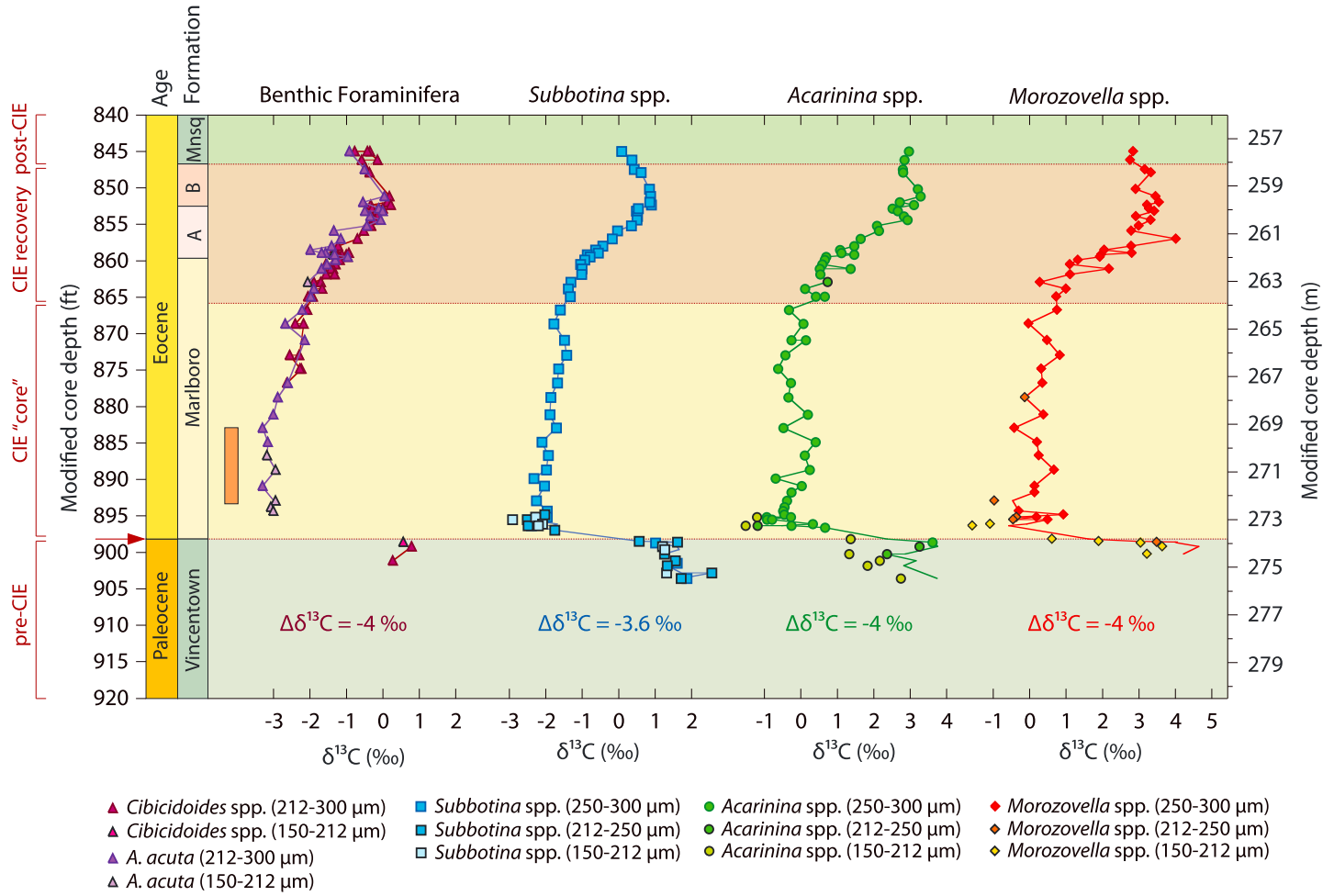

Figure 4. Monogeneric stable carbon isotope records of foraminifera at Millville. Samples from smaller size fractions (150–212 and 212–250 µm) are outlined in black, and solid lines represent the corrected for the test size $\delta^{13}C$ values. The orange vertical bar indicates a stable interval of the CIE "core" from which the average CIE "core" $\delta^{13}C$ value was estimated.

and Schaller, 2013] supported by our foraminiferal $\delta^{13}C$ data, the section has been divided into four intervals: (1) pre-CIE, (2) the CIE "core", (3) CIE recovery during which isotopic values returned to pre-CIE isotopic levels, and (4) post-CIE (Figure S1).

Our analyses show specific isotopic responses to the PETM in surface versus thermocline and benthic species. We define changes in $\delta^{13}C$ ($\Delta\delta^{13}C$) and $\delta^{18}O$ ($\Delta\delta^{18}O$) as differences between the average pre-CIE value and average value from the stable interval of the CIE "core" indicated by vertical bars in Figures 4 and 5. Most taxa show $\Delta\delta^{13}C$ of −4‰ following the CIE initiation with slightly lower *Subbotina* spp. $\Delta\delta^{13}C$ of −3.6‰ (Figure 4). Changes in $\delta^{18}O$ values vary among foraminifera: $\Delta\delta^{18}O$ in surface dwellers *Morozovella* spp. and *Acarinina* spp. are −1‰, whereas *Subbotina* spp. and benthic taxa show a larger $\Delta\delta^{18}O$ of −1.8‰ (Figure 5). The isotopic response of *Morozovella* spp. should be interpreted cautiously because of the limited data in the pre-CIE interval (six measurements within 60 cm below the CIE onset). However, we note that the pre-CIE $\delta^{13}C$ and $\delta^{18}O$ values in *Morozovella* spp. at Bass River [*Zachos et al.*, 2007; *John et al.*, 2008; *Babila et al.*, 2016] are similar to those at Millville, thus validating the Millville pre-CIE record (Figures 6, S2, and S3). The same is true for the benthic pre-CIE isotopic records.

To compare the isotopic responses of foraminifera across the PETM section at Millville, we present crossplots of $\delta^{18}O$ versus $\delta^{13}C$ for intervals representing pre-CIE, CIE "core", CIE recovery, and post-CIE (Figure S1). Below the CIE onset, the carbon isotopic gradient between surface and benthic species is ~3.0–3.5‰ and the oxygen isotopic gradient is ~1.75‰. *Morozovella* spp. have high $\delta^{13}C$ and low $\delta^{18}O$ values indicating calcification

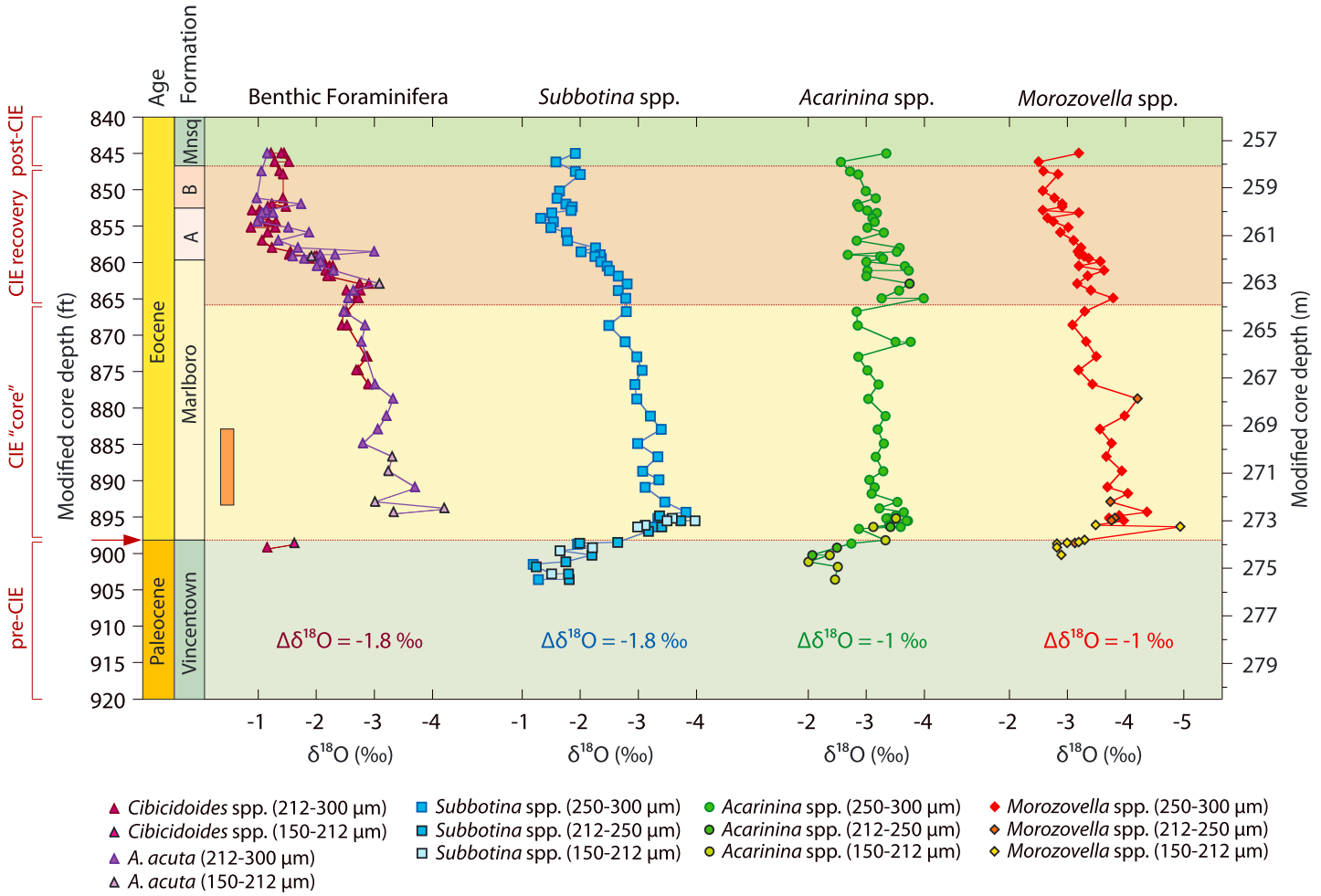

Figure 5. Monogeneric stable oxygen isotope records of foraminifera at Millville. Samples from smaller size fractions (150–212 and 212–250 µm) are outlined in black. The orange vertical bar indicates a stable interval of the CIE "core" from which the average CIE core $\delta^{18}O$ value was estimated.

in shallowest water column, *Subbotina* spp. have low $\delta^{13}C$ and high $\delta^{18}O$ and are deeper dwellers, and *Acarinina* spp. have isotopic values in between (however, closer to those of *Morozovella* spp.). Benthic species of *Cibicidoides* record bottom water conditions, and *G. beccariiformis* show the lowest $\delta^{13}C$ and highest $\delta^{18}O$ implying an infaunal habitat as suggested previously [e.g., *Katz et al.*, 2010]. We exclude *G. beccariiformis* from our interpretations of surface to bottom isotopic gradients because it is only found in the uppermost Paleocene (pre-CIE interval) and has an infaunal habitat.

In the CIE "core", the surface to thermocline to bottom $\delta^{13}C$ gradient is similar to the pre-CIE, whereas the vertical $\delta^{18}O$ gradient decreases to ~1‰. *Morozovella* spp. and *Acarinina* spp. record similar $\delta^{13}C$ values, and both are higher than thermocline dwelling *Subbotina* spp. and benthic foraminifera. *Morozovella* spp. continues to record the lowest $\delta^{18}O$ values, although *Acarinina* spp. are similar to $\delta^{18}O$ values in *Subbotina* spp. and benthic species of *Cibicidoides* and *A. acuta*. Post-CIE values of all taxa are similar to the pre-CIE values, with a return occurring through the recovery phase (Figure S1). Both the recovery and post-CIE intervals record reestablished surface to thermocline isotopic gradients with *Acarinina* spp. $\delta^{18}O$ values identical to those of *Morozovella* spp. (Figure S1).

4.2. Foraminiferal Isotopic Records From the New Jersey Paleoshelf

Water column gradients on the New Jersey paleoshelf were reconstructed using foraminiferal $\delta^{13}C$ and $\delta^{18}O$ to assess changes in hydrography and organic carbon cycling that may be associated with climate perturbation during the PETM (Figures 1, 6, S2, and S3). We use previously reported data from Bass River (~12 km

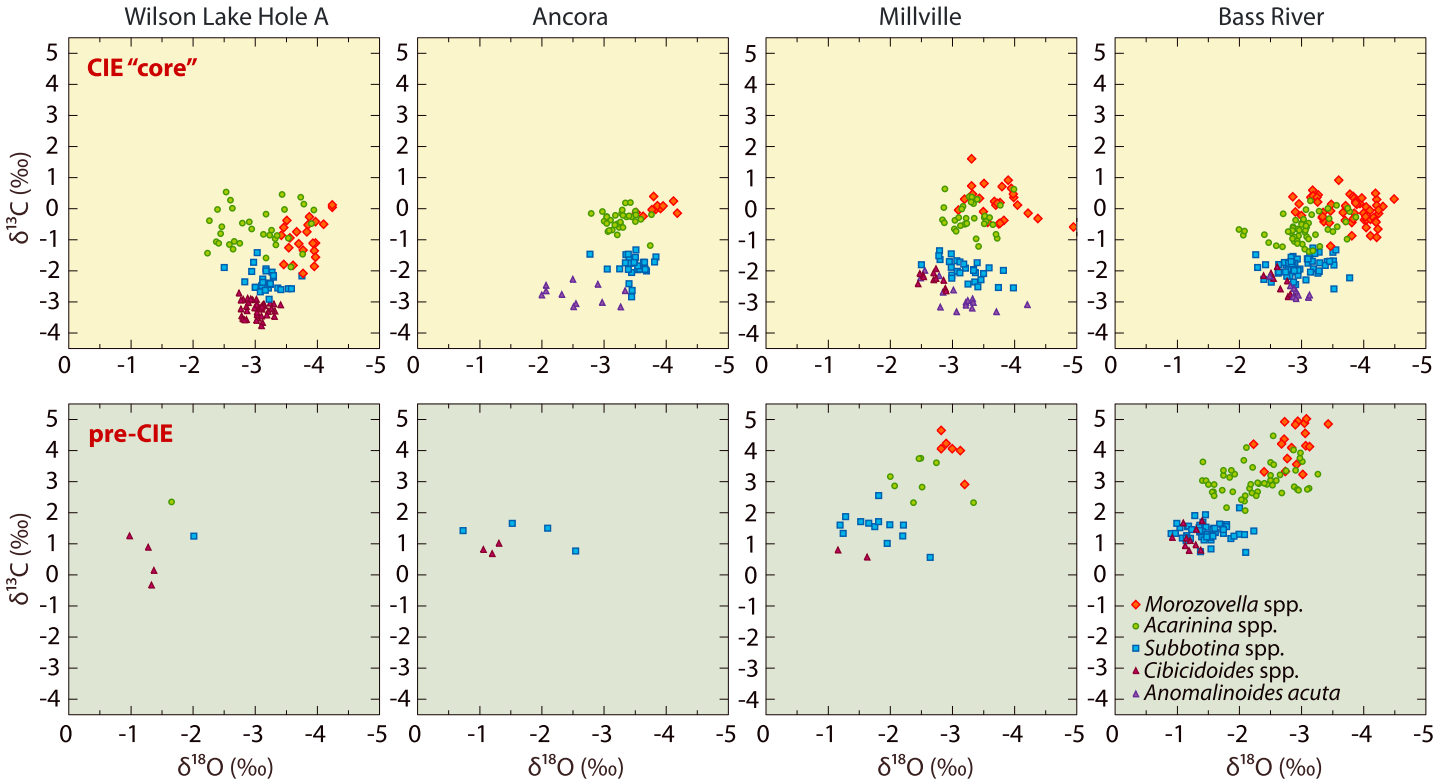

Figure 6. Planktonic and benthic foraminiferal crossplots of $\delta^{18}O$ versus $\delta^{13}C$ generated for the New Jersey coastal plain ODP sites Wilson Lake Hole A [*Zachos et al.*, 2006], Ancora [*Cramer and Kent*, 2005; *Babila*, 2014], Millville [this study], and Bass River [*Cramer et al.*, 1999; *Zachos et al.*, 2007; *John et al.*, 2008; *Babila et al.*, 2016]. Bottom plots show the surface to benthic foraminiferal isotopic gradients in the interval below the CIE onset, and top plots illustrate those in the CIE "core."

seaward) [*Cramer et al.*, 1999; *Zachos et al.*, 2007; *John et al.*, 2008; *Babila et al.*, 2016], Ancora (~16 km landward) [*Cramer and Kent*, 2005; *Babila*, 2014], and Wilson Lake Hole A (~23 km landward) [*Zachos et al.*, 2006] sites to summarize foraminiferal isotopic data in a series of crossplots representing intervals of the pre-CIE and CIE "core" deposition (Figure 6).

One concern about merging our data sets with previous published records is the difference in single versus multiple species analyses. Millville and Bass River are the only cores with a complete surface, thermocline, and benthic assemblage of foraminifera allowing reconstruction of $\delta^{13}C$ and $\delta^{18}O$ gradients below the CIE onset. Measurements of surface dwellers *Morozovella* spp. and *Acarinina* spp. below the CIE onset at Bass River were mostly done on single specimens [*Zachos et al.*, 2007], yielding higher variability in $\delta^{13}C$ and $\delta^{18}O$ values which likely reflects a seasonal signal and a range of actual environmental conditions. Isotopic measurements performed on multiple specimens at Millville exhibit less scatter and show a few intermediate $\delta^{13}C$ and $\delta^{18}O$ values across the CIE onset instead of bimodal isotopic distribution observed at Bass River (Figures S2 and S3). Specifically, most of intermediate values at Millville occur below the CIE onset within the Vincentown/Marlboro transitional interval and likely represent mixing of pre-CIE and CIE populations due to bioturbation/reworking (Figures 3 and 4).

Considering an average of the single-specimen data at Bass River, the carbon isotopic gradient between surface dwellers and benthic foraminifera below the CIE onset is ~3.0–3.5‰, with *Acarinina* spp. falling between *Morozovella* spp. and *Subbotina* spp. (Figures 6 and S2). In the CIE "core", the $\delta^{13}C$ surface to bottom gradients among all sites along the shelf remain the same value of ~3.0–3.5‰ (Figures 6 and S2). Through the entire CIE "core", surface dwellers *Morozovella* spp. and *Acarinina* spp. record similar $\delta^{13}C$ values, with *Morozovella* spp. being slightly more positive (Figures 6 and S2). The $\delta^{13}C$ vertical gradients derived from the Paleocene-Eocene foraminifera are consistent with $\delta^{13}C$ gradients previously reported for the Cretaceous-Eocene warm ocean at various locations [*Pearson et al.*, 2001; *Sexton et al.*, 2006; *John et al.*, 2013]. The observed $\delta^{13}C$ gradients are much greater than $\delta^{13}C$ vertical gradients in the modern ocean (<2‰) and have

been explained as evidence for more efficient biological pump in greenhouse worlds [*Hilting et al*., 2008; *John et al*., 2013].

All New Jersey cores show reductions in $\delta^{18}O$ vertical gradients in the CIE "core" compared to below the CIE onset (Figures 6 and S3). Below the CIE, the $\delta^{18}O$ gradient between *Morozovella* spp. and *Cibicidoides* spp. is ~1.75‰ based on records from Millville and Bass River (Figures 6 and S3). In the CIE "core", it decreases to ~1‰ in all four cores (Figures 6 and S3), being especially reduced in the lowest part of the "core" (Figure S3). *Acarinina* spp. display a change in the relative position in the surface to thermocline $\delta^{18}O$ gradient. Below the CIE onset, *Acarinina* spp. record $\delta^{18}O$ values that are between *Morozovella* spp. and *Subbotina* spp. (Figures 6 and S3). Above the CIE onset, *Acarinina* spp. show $\delta^{18}O$ values similar to those in *Subbotina* spp. at Bass River and Millville and even lower than in *Subbotina* spp. at more proximal sites Wilson Lake Hole A and Ancora (Figures 6 and S3). In the CIE recovery, *Acarinina* spp. $\delta^{18}O$ values sharply decrease by ~0.75‰ toward values similar to *Morozovella* spp. (Figure S3). This pattern in the $\delta^{18}O$ record of *Acarinina* spp. is recognized in the PETM sections of Millville and Bass River; the pattern is not seen at Wilson Lake Hole A and Ancora due to truncation of the recovery interval of the PETM section at these sites (Figure S3). This shift in *Acarinina* spp. $\delta^{18}O$ can be used as another characteristic of the recovery onset accompanying the returning trend in stable isotopes among all genera to pre-CIE isotopic levels.

5. Discussion

5.1. Environmental and Biotic Controls on Stable Isotope Records of Foraminifera

We examine two scenarios to explain different isotopic responses recorded by foraminifera in the PETM shelf records. The first makes a standard paleoceanographic assumption that ascribes isotopic differences to depth habitats of the different taxa (i.e., surface mixed layer versus thermocline dwellers versus benthic foraminifera). Implicit in this assumption is that the planktonic foraminiferal values reflect mean annual conditions. Therefore, changes in the differences among the different taxa must reflect reorganization of the hydrographic column. The second scenario allows for a change in habitat due to an environmental perturbation, which can be accomplished by changes in either the season of planktonic foraminiferal calcification or the depth at which they calcify. This scenario more accurately reflects the modern foraminiferal populations in the middle to high latitudes, where a succession of species grows throughout the spring bloom and into the summer [e.g., *Bé*, 1982; *Reynolds and Thunell*, 1985]. We also discuss the potential influences of symbiont loss and carbonate ion effect on foraminiferal stable isotope records in the supporting information.

We reconstruct the New Jersey paleoslope following *Esmeray-Senlet et al*. [2015] for four sites: Wilson Lake, Ancora, Millville, and Bass River (Figure 7). Figure 7a demonstrates the hydrography of the New Jersey paleoshelf prior the CIE onset, whereas Figures 7b and 7c illustrate the hydrographic conditions after the CIE onset, each representing the proposed mechanisms. To characterize paleoshelf hydrography, we plot $\delta^{18}O$ gradients in the water column for all sites based on average $\delta^{18}O$ values of *Morozovella* spp., *Acarinina* spp., *Subbotina* spp., *Cibicidoides* spp., and *A. acuta*. Small insets on the right indicate the water column on the modern New Jersey shelf after *Castelao et al*. [2010] with the seasonal thermal structure and thus $\delta^{18}O$ gradients in June and October that we used as analogs (Figure 7).

Based on the different $\delta^{18}O$ changes recorded among the foraminiferal taxa, we suggest that the thermocline deepened on the shelf after the CIE onset, responding to warming (scenario 1; Figure 7b). Under this scenario, the surface-mixed taxa (*Morozovella* and *Acaranina*) record the mean surface temperature change of ~5°C ($\Delta\delta^{18}O = -1‰$) with greater warming in the thermocline and benthic taxa of 8 to 9°C ($\Delta\delta^{18}O = -1.75‰$). Persistent warming during the PETM would propagate heat into deeper layers and create a more homogenous water column with a thicker warm mixed layer and a deeper, more gradual thermocline. This is similar in nature to hydrographic changes observed on the modern New Jersey shelf with a thinner mixed layer in summer and a thicker mixed layer with a deeper and more gradual seasonal thermocline in fall (Figure 7, insets). Today, the surface ocean stores heat for the entire summer resulting in a strong seasonal thermocline that breaks down to a more homogenous water column structure in the fall as a result of cooling and increased storm activity [*Castelao et al*., 2010]. Assuming a relatively constant depth habitat of planktonic foraminifera, a more gradual thermocline during the CIE "core" would explain such different $\delta^{18}O$ responses in surface dwellers versus thermocline dwelling and benthic foraminifera (Figure 7b).

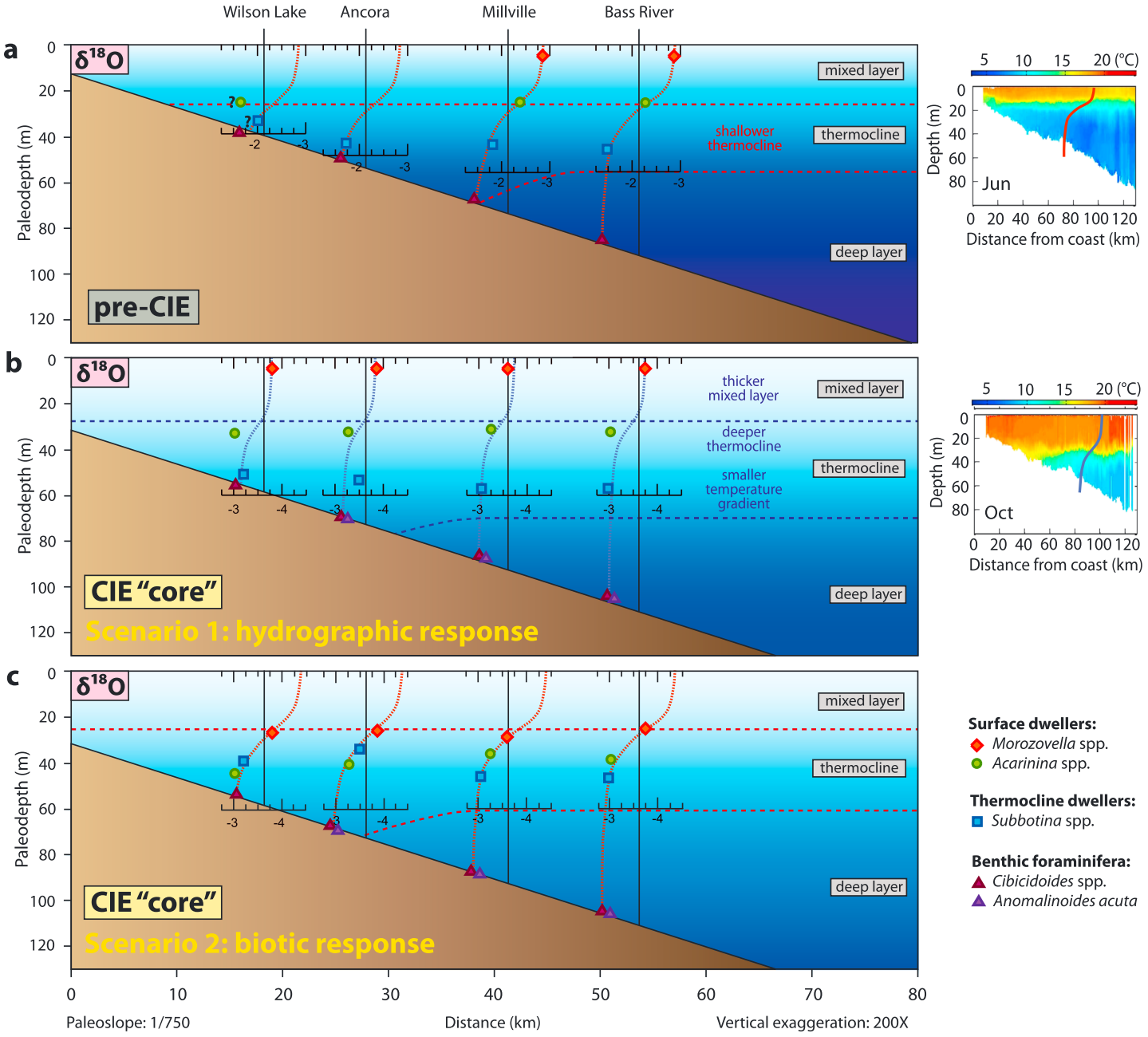

Figure 7. Hydrographic reconstruction of the New Jersey paleoshelf for the periods of (a) pre-CIE and (b and c) CIE "core" deposition. Figures 7b and 7c illustrate two scenarios explaining different isotopic response in surface versus thermocline dwellers after the CIE onset: Figure 7b—change in the water column structure and Figure 7c—change in habitat of the surface dwellers. Red and blue lines represent the $\delta^{18}O$ gradients drawn for each site with single-genus average $\delta^{18}O$ values plotted on top. Foraminiferal $\delta^{18}O$ data are from Wilson Lake Hole A [*Zachos et al.*, 2006], Ancora [*Babila*, 2014; *Cramer and Kent*, 2005], Millville [this study], and Bass River [*Cramer et al.*, 1999; *Zachos et al.*, 2007; *John et al.*, 2008; *Babila et al.*, 2016]. Paleoslope reconstruction is modified for the PETM after *Esmeray-Senlet et al.* [2015]. Plots on the right show the thermal structure of the water column across the modern New Jersey shelf in June and October [*Castelao et al.*, 2010].

A change in the water column structure during the PETM is a plausible mechanism to explain isotopic trends in planktonic foraminifera observed on the shelf. A global temperature rise of 4–8°C [e.g., *Dunkley Jones et al.*, 2013] and a possible increase in mixing and storm activity due to an enhanced tropical heat and moisture transport during the PETM [e.g., *Caballero and Langen*, 2005; *Pagani et al.*, 2006; *Carmichael et al.*, 2016] would produce a deeper, more gradual thermocline. However, a few centuries to thousands of years after the initial warming, establishment of equilibrium conditions would require restoration of the thermocline structure

similar to the pre-CIE. Sustainability of hydrographic changes during the CIE would require either a freshwater input initiating stratification [*Stassen et al*., 2015] or a decrease in the meridional thermal gradient that would have caused more warming in thermocline waters globally. Proxy data for the sea surface [e.g., *Sluijs et al*., 2006; *Bijl et al*., 2009; *Sluijs et al*., 2011; *Frieling et al*., 2014] and mean air [*Weijers et al*., 2007] temperatures indicate amplified warming in the Arctic region and the Southern Ocean, suggesting strongly reduced meridional temperature gradient during the PETM. Furthermore, model simulations for the Eocene period of global warmth also predict polar amplification where higher latitudes experience greater warming than low latitudes [*Huber and Caballero*, 2003, 2011; *Lunt et al*., 2012]. Suggested polar amplification would have caused reorganization of the thermocline globally until meridional temperature gradient restored to the pre-CIE state. The reduced to 1‰ $\delta^{18}O$ vertical gradient during the PETM, i.e., decreased thermal gradient on the paleoshelf, is consistent with a reduced meridional thermal gradient and polar amplification.

The second scenario considers that planktonic foraminifera may have responded differently to environmental perturbations associated with the PETM onset by changing their depth habitat and/or season of dominant calcification. Surface dwellers (*Morozovella* and *Acarinina* spp.) may have migrated out of the surface mixed layer due to inhospitable conditions (e.g., high temperature, lower salinity, and intense acidification) (scenario 2; Figure 7c). In this scenario, the mixed layer in contact with the PETM atmosphere was too warm, fresh, or corrosive, forcing surface dwellers to descend into cooler, saltier, and possibly more buffered thermocline waters. Both of the surface mixed taxa either descended deeper in the water column or "bloomed" earlier in the season; thus, *Morozovella* spp. and *Acarinina* spp. $\delta^{18}O$ values record the PETM warming minus the change in habitat cooling (Figure 7c). Accordingly, $\delta^{13}C$ values would reflect the whole ocean reservoir decrease plus a change in habitat. It is, however, possible that the variable isotopic responses also reflect a shift in bloom seasons and not just depth migration. Furthermore, one could interpret the $\delta^{13}C$ in terms of warm, nutrient-depleted water during the summer months (e.g., *Morozovella*) and lower $\delta^{13}C$ associated with spring upwelling (e.g., *Subbotina*).

To test the idea that acidification was the environmental driver for the depth migration of planktonic foraminifera, we use estimates of surface ocean acidification from recent boron-based proxy records [*Penman et al*., 2014; *Babila et al*., 2016]. Studies from both the North Pacific [*Penman et al*., 2014] and paleoshelf of New Jersey [*Babila et al*., 2016] show a decrease of ~0.3–0.4 pH units in both surface and thermocline waters. If acidification is a possible environmental stress to planktonic foraminifera it seems unlikely that migration to more corrosive thermocline waters would occur. Conversely, B/Ca and $\delta^{18}O$ records of surface-dwelling *Acarinina* spp. and thermocline dwelling *Subbotina* spp. indicate similar pH and $\delta^{18}O$ values, respectively, recorded by these taxa after the CIE onset (Figures 3, 6, and S3). This means that *Acarinina* spp. might have occupied the same niche in the water column as *Subbotina* spp. during the CIE "core" phase and then possibly migrated back to the mixed layer during the recovery phase.

Another possible reason for surface dwellers migration deeper into the water column could be due to the freshening of the mixed layer. Although individual species of foraminifera can tolerate and reproduce in cultures in salinities as low as 20 practical salinity unit (psu) and over 40 psu [*Bijma et al*., 1990; *Spindler*, 1996], robust assemblages of planktonic foraminifera are restricted to salinities greater than 30 psu [*Bé and Tolderlund*, 1971; *Bijma et al*., 1990]. Similarly, although *r*-selected coccolithophroidae such as *Emiliani huxleyi* tolerate nearshore, low-salinity environments [e.g., *Fisher and Honjo*, 1989], diverse nannoplankton assemblages such as those found in Wilson Lake [*Gibbs et al*., 2006a], Millville, and Bass River [*Kahn and Aubry*, 2004; *Harris*, 2010] are restricted to normal marine salinities (e.g., $>$32 psu) [*Menschel et al*., 2016].

An enhanced hydrological cycle during the PETM [e.g., *Pagani et al*., 2006; *Kopp et al*., 2009] would have triggered greater river discharge and resulted in formation of a freshwater lens at the sea surface. Previous studies have suggested a modest freshening (up to 3–4 psu) of surface waters on New Jersey paleoshelf during the PETM [*Zachos et al*., 2006], although this result requires verification due to sparse pre-CIE isotopic data and will be subject of the subsequent study [*Makarova et al*., 2013]. A low-salinity anomaly associated with a freshwater lens at the top would be inhospitable pushing the mixed layer dwellers deeper into the water column. Following *Kopp et al.'s* [2009] suggestion of an Appalachian Amazon development on the mid-Atlantic shelf, we use the modern Amazon salinity variability on the shelf as an analog. The Amazon plume extends up to 80–250 km offshore and causes sea surface salinities (SSSs) in the upper 5–10 m water column to drop

below 33 psu [*Lentz and Limeburner*, 1995; *Geyer et al*., 1996]. A smaller-scale river system would probably not lower SSS as much and as far offshore as the Amazon-type river system. For example, Hudson River runoff lowers SSS in the upper 10–15 m by only 1 psu during spring and summer [*Castelao et al*., 2010]. Nevertheless, even in the heart of the modern Amazon low-salinity lens, effects on the shelf in water depths greater than 20 m (100 km from shore) are limited to the top few meters [*Lentz and Limeburner*, 1995], allowing us to reject the hypothesis that surface dwellers were forced by freshwater into the thermocline.

Development of the river-dominated drainage system on the mid-Atlantic shelf during the PETM might have affected bottom salinities as well. *Powars and Edwards* [2015] suggest that the Marlboro Formation represents delta front turbidites and/or wave-enhanced sediment gravity flows. Similarly, most of fine sediments deposited on the Amazon shelf are transported at the bottom in form of fluid mud [*Lentz and Limeburner*, 1995; *Geyer et al*., 1996]. Fluid muds decrease near-bottom salinities to 28–30 psu within the lower 2–3 m of the water column on the Amazon shelf, but they do not affect bottom salinity at deeper than 20 m isobaths where the shelf deep waters are constant at normal marine salinities [*Lentz and Limeburner*, 1995; *Geyer et al*., 1996]. Therefore, bottom gravity flows of mud on the mid-Atlantic shelf during the PETM would not have affected bottom salinity nor would they have created a larger $\delta^{18}O$ decrease in benthic foraminifera across the CIE onset. Moreover, analyses of benthic foraminiferal assemblages from the New Jersey paleoshelf show abundant benthic foraminifera in the CIE "core" despite the turnover across the P/E boundary [*Cramer et al*., 1999; *Harris et al*., 2010; *Stassen et al*., 2012]. A detailed recent study by *Stassen et al*. [2015] indicates an overall decrease in benthic foraminiferal abundances and prevalence of stress-tolerant taxa after the CIE onset, suggesting water column stratification and oxygen depletion and eutrophication of the bottom waters. Based on benthic foraminiferal biofacies that indicate a response to productivity and oxygen levels, we conclude that gravity flows did not stress benthic assemblage by freshening (i.e., not affecting $\delta^{18}O$) or by changing the clarity of bottom seawater.

Although we cannot exclude scenario 2, the similar $\delta^{13}C$ changes in all foraminifera across the shelf argue against a change in depth habitats, unless there was a change in bloom season. If the surface dwellers were forced out of the mixed layer, they would record lower $\delta^{13}C$ values resulting in reduced $\delta^{13}C$ surface to bottom gradient. Instead, our stable isotopic records show a similar (3.6–4.0‰) magnitude of CIE among all taxa, challenging the migration scenario (Figures 4 and S2). Maintenance of the same $\delta^{13}C$ vertical gradient between surface dwellers and deep/benthic foraminifera suggests no major change in organic matter cycling on the shelf through the CIE and that foraminifera maintained their vertical habitat distribution with a weakened thermocline structure or change the season of calcification.

Scenario 2 could still be valid if there was change in bloom season. Extremely high-summer sea surface temperatures (SSTs) could have precluded calcification of surface dwellers during the summer months and restricted calcification to the cooler times of the year. Thus, the reduced $\Delta\delta^{18}O$ reflects the inability of the surface-dwelling foraminifera to calcify in summer, hence shifting the population to cooler temperatures and higher $\delta^{18}O$ values, although they continued to calcify in nutrient-depleted surface waters explaining the similar $\delta^{13}C$ changes. In this scenario, the true temperature change on the paleoshelf was on the order of 8 to 9°C (recorded by the thermocline and benthic taxa). In the modern ocean, 33°C is an upper limit on planktonic foraminiferal calcification [*Bijma et al*., 1990]. Given these constraints, it is not expected that surface-dwelling planktonic foraminifera would be able to calcify in the warmest parts of the year if temperature change in coast surface waters was on the order of 8–9°C, exceeding temperatures of 33°C [*Zachos et al*., 2006; *Sluijs et al*., 2007; *Makarova et al*., 2013].

A 8–9°C warming during the PETM on shelf is higher than observed for open ocean low- to middle-latitude sites [e.g., *Bralower et al*., 1995; *Zachos et al*., 2003; *Tripati and Elderfield*, 2004; *Hollis et al*., 2015]. We note that in coastal regions, the proximity to land and the shallow water depths produce larger seasonal changes in temperature relative to the open ocean. *Climate: Long-Range Investigation, Mapping, and Prediction Project Members* [1976, 1981] also demonstrated that coastal regions recorded larger temperature changes relative to the open ocean under different climate conditions. The paleoshelf setting allows us to distinguish between different scenarios. However, the observation that planktonic foraminiferal on the shelf may have had a similar upper temperature limit ($<$35°C) means that planktonic foraminifera in tropical and subtropical ocean must have responded in kind and did not record the full range of SST warming due to their temperature limits during the PETM.

5.2. Environmental Response of Other Plankton

The biotic and ecological responses of other groups of planktonic organisms, calcareous nannofossils and dinoflagellates, provide useful insights to planktonic foraminiferal responses. Studies of calcareous nannofossils from various locations, both open ocean and shelf, have suggested significant shifts in assemblages associated with global turnover [e.g., *Bralower*, 2002; *Tremolada and Bralower*, 2004; *Gibbs et al*., 2006a; *Bown and Pearson*, 2009; *Self-Trail et al*., 2012]. *Gibbs et al*. [2006b] noted the co-occurrence of fragile and heavily calcified forms of coccolithophorids in PETM sections, suggesting no crash of calcification in the upper water column. Despite surface ocean acidification associated with the PETM onset [*Penman et al*., 2014; *Babila et al*., 2016], most studies agree that acidification did not affect production of calcareous nannofossils but rather elevated temperature and/or nutrients did [e.g., *Bralower*, 2002; *Tremolada and Bralower*, 2004; *Gibbs et al*., 2006a; *Bown and Pearson*, 2009; *Gibbs et al*., 2010; *Self-Trail et al*., 2012]. In contrast to the nutrient-depleted, thermally stratified open ocean gyres, shelf areas show increased productivity [*Bralower*, 2002; *Gibbs et al*., 2006a; *Self-Trail et al*., 2012] that is also supported by elevated Sr/Ca ratios in coccolithophores [*Stoll et al*., 2007]. Whereas some species on the shelf adapted to warm-water, eutrophic conditions in the upper water column [e.g., *Self-Trail et al*., 2012], malformed ecophenotypes of the excursion taxa *Discoaster* and *Rhomboaster* [*Aubry*, 1998; *Kahn and Aubry*, 2004] might have migrated lower in the photic zone near the nutricline. *Bralower and Self-Trail* [2016] suggested that migration of the excursion species into a deeper habitat with lower carbonate saturation levels due to remineralization of organic matter resulted in their malformation. They also proposed that *Discoaster* spp. occupied a deeper habitat near the nutricline as a result of the expansion of a lower photic zone niche caused by warming and increased stratification, whereas normal calcareous nannoplankton assemblages characterized the upper photic zone.

Similar to the perturbations observed in calcareous nannofossil assemblages, records of dinoflagellate cysts document abrupt, global biotic changes across the PETM [e.g., *Powell et al*., 1996; *Bujak and Brinkhuis*, 1998; *Crouch et al*., 2001, 2003; *Iakovleva et al*., 2001; *Sluijs et al*., 2006, 2007; *Sluijs and Brinkhuis*, 2009]. The most prominent response associated with the PETM/CIE is the rapid, synchronous onset of the *Apectodinium*-dominated assemblages (acme) observed ubiquitously [e.g., *Bujak and Brinkhuis*, 1998; *Crouch et al*., 2001; *Sluijs and Brinkhuis*, 2009]. Most studies suggest that the increase in *Apectodinium* abundances is associated with significantly higher sea surface temperatures (SSTs) and increased surface water productivity (eutrophication) [*Bujak and Brinkhuis*, 1998; *Sluijs and Brinkhuis*, 2009]. However, dinocyst distribution from the New Jersey paleoshelf may also indicate low salinity and/or changes in water column stratification affecting *Apectodinium* abundances [*Sluijs et al*., 2007; *Sluijs and Brinkhuis*, 2009]. As we show here, both planktonic foraminiferal and nannofossil assemblages suggest a limited change in salinity, but do suggest a change in water column stratification and chemistry, consistent with the dinoflagellate response.

Overall, studies of calcareous nannofossils and dinoflagellates suggest that elevated temperatures, increased productivity, and water column stratification influenced phytoplankton abundances in the coastal regions during the PETM. Some species went into the deep photic zone as refuge to escape stressful conditions in the surface ocean, and some formed extreme morphotypes as adaptation to harsh environments. Surface-dwelling foraminifera *Morozovella* and *Acarinina* also developed excursion taxa that presumably occupied a deep habitat during the PETM [*Kelly et al*., 1998]. However, the species of *Morozovella* and *Acarinina* reported here are not the excursion foraminifera and planktonic foraminiferal excursion taxa, though present, are not dominant. The proposed migration of the surface dwellers into a deeper habitat (scenario 2) should require their ability to tolerate the twilight zone. Sufficient light level might be critical since both *Morozovella* and *Acarinina* are symbiont-bearing genera that maintained photosynthetic symbionts during the PETM (see discussion of bleaching in the supporting information).

6. Conclusions

We present new stable isotopic data from planktonic and benthic foraminifera at Millville, NJ, and compare these data to other New Jersey coastal plain cores. Our comparisons show a similar isotopic response in foraminifera across the CIE onset on the mid-Atlantic shelf: an ~4‰ decrease in $\delta^{13}C$ values in all taxa and a larger $\Delta\delta^{18}O$ in thermocline dwelling and benthic foraminifera than in surface dwellers. Such isotopic responses are also expressed in constant $\delta^{13}C$ and reduced $\delta^{18}O$ vertical gradients between surface, thermocline dwelling, and benthic foraminifera in the CIE "core". To explain this we propose two scenarios. Scenario

1 posits a change in water column structure: surface and thermocline dwellers kept the same depth in the water column, but they record the signal of a thicker warm mixed layer and a deeper, more gradual thermocline. Scenario 2 posits a change in the habitat of the surface dwellers due to environmental stress in the mixed layer or a shift to a cooler calcification season. In the first scenario, amplified warming in the thermocline waters sustained during the CIE "core" stage resulted from a reduction in the meridional thermal gradient. We eliminate changing pH and salinity as major environmental stressors, but others such as temperature and nutrient level might have affected surface dwellers to change their depth habitat or calcification season. Although we cannot exclude scenario 2, the similar $\delta^{13}C$ changes in all foraminifera across the shelf argue against migration of the surface-dwelling taxa deeper into the thermocline.

Acknowledgments
The data and supporting tables and figures are in the supporting information. This research was supported by ExxonMobil Russian Scholarship and excellence fellowship for doctoral research from the Graduate School New Brunswick, Rutgers University, awarded to M. Makarova. T. Babila acknowledges support by the National Science Foundation (NSF OISE-1107787), Schlanger Ocean Drilling Fellowship, and Joanna Resig Foraminiferal Research Fellowship. M. Makarova and J. Park thank Summer Aresty Program for the support of benthic foraminiferal analysis. We are grateful to R.K. Olsson for the advice on foraminiferal taxonomy and J.V. Browning for the comments. We thank R.A. Mortlock and N. Abdul for their help with stable isotope analyses and P. Darias for the assistance in sample preparation. Samples were provided by International Ocean Discovery Program Rutgers Core Repository supported by NSF grant OCE14-63759 (to K. Miller). We thank H. Pälike and two anonymous reviewers for their reviews and improvement of this manuscript.

References

Anagnostou, E., E. H. John, K. M. Edgar, G. L. Foster, A. Ridgwell, G. N. Inglis, R. D. Pancost, D. J. Lunt, and P. N. Pearson (2016), Changing atmospheric CO_2 concentration was the primary driver of early Cenozoic climate, *Nature*, *533*(7603), 380–384, doi:10.1038/nature17423.

Aubry, M.-P. (1998), Early Paleogene calcareous nannoplankton evolution: A tale of climatic amelioration, in *Late Paleocene-Early Eocene Climatic and Biotic Events in the Marine and Terrestrial Records*, edited by M.-P. Aubry, S. G. Lucas, and W. A. Berggren, pp. 158–203, Columbia Univ. Press, New York.

Aubry, M.-P., K. Ouda, C. Dupuis, W. A. Berggren, J. A. Van Couvering, and the Members of the Working Group on the Paleocene/Eocene Boundary (2007), The Global Standard Stratotype-section and Point (GSSP) for the base of the Eocene Series in the Dababiya section (Egypt), *Episodes*, *30*(4), 271–286.

Babila, T. L. (2014), Boron/calcium in planktonic foraminifera: Proxy development and application to the Paleocene-Eocene boundary, PhD thesis, 140 p., Rutgers Univ., N. J.

Babila, T. L., Y. Rosenthal, J. D. Wright, and K. G. Miller (2016), A continental shelf perspective of ocean acidification and temperature evolution during the Paleocene-Eocene Thermal Maximum, *Geology*, *44*(4), 275–278, doi:10.1130/G37522.1.

Bains, S., R. M. Corfield, and R. D. Norris (1999), Mechanisms of climate warming at the end of the Paleocene, *Science*, *285*, 724–727.

Bé, A. W. H. (1960), Ecology of recent planktonic foraminifera: Part 2—Bathymetric and seasonal distributions in the Sargasso Sea off Bermuda, *Micropaleontology*, *6*(4), 373–392.

Bé, A. W. H. (1982), Biology of planktonic foraminifera, in *Foraminifera: Notes for a Short Course, University of Tennessee, Studies in Geology*, vol. 6, edited by T. W. Broadhead, pp. 51–89, Knoxville, Tenn.

Bé, A. W. H., and D. S. Tolderlund (1971), Distribution and ecology of living planktonic foraminifera in surface waters of the Atlantic and Indian Oceans, *Micropaleontol. Oceans*, 105–149.

Berggren, W. A., and J. Aubert (1975), Paleocene benthonic foraminiferal biostratigraphy, paleobiogeography and paleoecology of Atlantic-Tethyan regions: Midway-type fauna, *Palaeogeogr. Palaeoclimatol. Palaeoecol.*, *18*, 73–192.

Bijl, P. K., S. Schouten, A. Sluijs, G.-J. Reichart, J. C. Zachos, and H. Brinkhuis (2009), Early Palaeogene temperature evolution of the southwest Pacific Ocean, *Nature*, *461*, 776–779, doi:10.1038/nature08399.

Bijma, J., W. W. Faber Jr., and C. Hemleben (1990), Temperature and salinity limits for growth and survival of some planktonic foraminifers in laboratory cultures, *J. Foraminiferal Res.*, *20*(2), 95–116.

Birch, H. S., H. K. Coxall, and P. N. Pearson (2012), Evolutionary ecology of early Paleocene planktonic foraminifera: Size, depth habitat and symbiosis, *Paleobiology*, *38*(3), 374–390.

Boersma, A., I. Premoli Silva, and N. J. Shackleton (1987), Atlantic Eocene planktonic foraminiferal paleohydrographic indicators and stable isotope paleoceanography, *Paleoceanography*, *2*(3), 287–331, doi:10.1029/PA002i003p00287.

Bornemann, A., and R. D. Norris (2007), Size-related stable isotope changes in Late Cretaceous planktic foraminifera: Implications for paleoecology and photosymbiosis, *Mar. Micropaleontol.*, *65*, 32–42.

Bowen, G. J., B. J. Maibauer, M. J. Kraus, U. Röhl, T. Westerhold, A. Steimke, P. D. Gingerich, S. L. Wing, and W. C. Clyde (2015), Two massive, rapid releases of carbon during the onset of the Palaeocene–Eocene Thermal Maximum, *Nat. Geosci.*, *8*, 44–47, doi:10.1038/NGEO2316.

Bown, P., and P. Pearson (2009), Calcareous plankton evolution and the Paleocene/Eocene Thermal Maximum event: New evidence from Tanzania, *Mar. Micropaleontol.*, *71*, 60–70, doi:10.1016/j.marmicro.2009.01.005.

Bralower, T. J. (2002), Evidence for surface water oligotrophy during the Paleocene-Eocene Thermal Maximum: Nannofossil assemblage data from Ocean Drilling Program Site 690, Maud Rise, Weddell Sea, *Paleoceanography*, *17*(2), 1023, doi:10.1029/2001PA000662.

Bralower, T. J., and J. M. Self-Trail (2016), Nannoplankton malformation during the Paleocene-Eocene Thermal Maximum and its paleoecological and paleoceangraphic significance, *Paleoceanography*, *31*, 1423–1439, doi:10.1002/2016PA002980.

Bralower, T. J., J. C. Zachos, E. Thomas, M. Parrow, C. K. Paull, D. C. Kelly, I. Premoli Silva, W. V. Sliter, and K. C. Lohmann (1995), Late Paleocene to Eocene paleoceanography of the equatorial Pacific Ocean: Stable isotopes recorded at Ocean Drilling Program Site 865, Allison Guyot, *Paleoceanography*, *10*, 841–865, doi:10.1029/95PA01143.

Bralower, T. J., D. C. Kelly, S. Gibbs, K. Farley, L. Eccles, T. L. Lindemann, and G. J. Smith (2014), Impact of dissolution on the sedimentary record of the Paleocene–Eocene Thermal Maximum, *Earth Planet. Sci. Lett.*, *401*, 70–82, doi:10.1016/j.epsl.2014.05.055.

Bujak, J. P., and H. Brinkhuis (1998), Global warming and dinocyct changes across the Paleocene-Eocene epoch boundary, in *Late Paleocene-Early Eocene Climatic and Biotic Events in the Marine and Terrestrial Records*, edited by M.-P. Aubry, S. G. Lucas, and W. A. Berggren, pp. 277–295, Columbia Univ. Press, New York.

Caballero, R., and P. L. Langen (2005), The dynamic range of poleward energy transport in an atmospheric general circulation model, *Geophys. Res. Lett.*, *32*, L02705, doi:10.1029/2004GL021581.

Carmichael, M. J., et al. (2016), A model–model and data–model comparison for the early Eocene hydrological cycle, *Clim. Past*, *12*, 455–481, doi:10.5194/cp-12-455-2016.

Castelao, R., S. Glenn, and O. Schofield (2010), Temperature, salinity, and density variability in the central Middle Atlantic Bight, *J. Geophys. Res.*, *115*, C10005, doi:10.1029/2009JC006082.

CLIMAP Project Members (1976), The surface of the ice-age Earth, *Science*, *191*(4232), 1131.

CLIMAP Project Members (1981), *Seasonal Reconstructions of the Earth's Surface at the Last Glacial Maximum*, Geol. Soc. Am. Map Chart Ser. MC-36, Boulder, Colo.

Coxall, H. K., P. N. Pearson, N. J. Shackleton, and M. A. Hall (2000), Hantkeninid depth adaptation: An evolving life strategy in a changing ocean, *Geology*, *28*(1), 87–90.
Cramer, B. S., and D. V. Kent (2005), Bolide summer: The Paleocene/Eocene Thermal Maximum as a response to an extraterrestrial trigger, *Palaeogeogr. Palaeoclimatol. Palaeoecol.*, *224*, 144–166.
Cramer, B. S., M.-P. Aubry, K. G. Miller, R. K. Olsson, J. D. Wright, and D. V. Kent (1999), An exceptional chronologic, isotopic, and clay mineralogic record at the latest Paleocene Thermal Maximum, Bass River, NJ, ODP 174AX, *Bull. Soc. Geol. Fr.*, *170*(6), 883–897.
Crouch, E. M., C. Heilmann-Clausen, H. Brinkhuis, H. E. G. Morgans, K. M. Rogers, H. Egger, and B. Schmitz (2001), Global dinoflagellate event associated with the late Paleocene Thermal Maximum, *Geology*, *29*(4), 315–318.
Crouch, E. M., G. R. Dickens, H. Brinkhuis, M.-P. Aubry, C. J. Hollis, K. M. Rogers, and H. Visscher (2003), The *Apectodinium* acme and terrestrial discharge during the Paleocene-Eocene Thermal Maximum: New palynological, geochemical and calcareous nannoplankton observations at Tawanui, New Zealand, *Palaeogeogr. Palaeoclimatol. Palaeoecol.*, *194*, 387–403.
Cui, Y., L. R. Kump, A. J. Ridgwell, A. J. Charles, C. K. Junium, A. F. Diefendorf, K. H. Freeman, N. M. Urban, and I. C. Harding (2011), Slow release of fossil carbon during the Palaeocene–Eocene Thermal Maximum, *Nat. Geosci.*, *4*, 481–485, doi:10.1038/NGEO1179.
Curry, W. B., R. C. Thunell, and S. Honjo (1983), Seasonal changes in the isotopic composition of planktonic foraminifera collected in Panama Basin sediment traps, *Earth Planet. Sci. Lett.*, *64*, 33–43.
Cushman, J. A. (1951), *Paleocene Foraminifera of the Gulf Coastal Region of the United States and Adjacent Areas*, *Geol. Surv. Prof. Pap.*, vol. 232, pp. 1–75, United States Government Printing Office, Washington, D. C.
D'Hondt, S., and J. C. Zachos (1993), On stable isotopic variation and earliest Paleocene planktonic foraminifera, *Paleoceanography*, *8*(4), 527–547, doi:10.1029/93PA00952.
D'Hondt, S., J. C. Zachos, and G. Schultz (1994), Stable isotopic signals and photosymbiosis in late Paleocene planktic foraminifera, *Paleobiology*, *20*, 391–406.
Deuser, W. G., and E. H. Ross (1989), Seasonally abundant planktonic foraminifera of the Sargasso Sea: Succession, deep-water fluxes, isotopic compositions, and paleoceanographic implications, *J. Foraminiferal Res.*, *19*(4), 268–293.
Dickens, G. R., M. M. Castillo, and J. C. G. Walker (1997), A blast of gas in the latest Paleocene: Simulating first-order effects of massive dissociation of oceanic methane hydrate, *Geology*, *25*(3), 259–262.
Dunkley Jones, T., D. J. Lunt, D. N. Schmidt, A. Ridgwell, A. Sluijs, P. J. Valdes, and M. Maslin (2013), Climate model and proxy data constraints on ocean warming across the Paleocene-Eocene Thermal Maximum, *Earth Sci. Rev.*, *125*, 123–145, doi:10.1016/j.earscirev.2013.07.004.
Emiliani, C. (1954), Depth habitats of some species of pelagic foraminifera as indicated by oxygen isotope ratios, *Am. J. Sci.*, *252*(3), 149–158, doi:10.2475/ajs.252.3.149.
Epstein, S., R. Buchsbaum, H. Lowenstam, and H. Urey (1953), Revised carbonate-water isotopic temperature scale, *Geol. Soc. Am. Bull.*, *64*(11), 1315–1325.
Esmeray-Senlet, S., J. D. Wright, R. K. Olsson, K. G. Miller, J. V. Browning, and T. M. Quan (2015), Evidence for reduced export productivity following the Cretaceous/Paleogene mass extinction, *Paleoceanography*, *30*, 718–738, doi:10.1002/2014PA002724.
Fairbanks, R. G., and P. H. Wiebe (1980), Foraminifera and chlorophyll maximum: Vertical distribution, seasonal succession, and paleoceanographic significance, *Science*, *209*, 1524–1526.
Fairbanks, R. G., M. Sverdlove, R. Free, P. H. Wiebe, and A. W. H. Bé (1982), Vertical distribution and isotopic fractionation of living planktonic foraminifera in the Panama Basin, *Nature*, *298*, 841–844.
Fisher, N. S., and S. Honjo (1989), Intraspecific differences in temperature and salinity responses in the coccolithophore *Emiliania huxleyi*, *Biol. Oceanogr.*, *6*(3–4), 355–361.
Frieling, J., A. I. Iakovleva, G. J. Reichart, G. N. Aleksandrova, Z. N. Gnibidenko, S. Schouten, and A. Sluijs (2014), Paleocene–Eocene warming and biotic response in the epicontinental West Siberian Sea, *Geology*, *42*(9), 767–770, doi:10.1130/G35724.1.
Geyer, W. R., R. C. Beardsley, S. J. Lentz, J. Candela, R. Limeburner, W. E. Johns, B. M. Castro, and I. D. Soares (1996), Physical oceanography of the Amazon shelf, *Cont. Shelf Res.*, *16*(5/6), 575–616.
Gibbs, S. J., H. M. Stoll, P. R. Bown, and T. J. Bralower (2010), Ocean acidification and surface water carbonate production across the Paleocene–Eocene Thermal Maximum, *Earth Planet. Sci. Lett.*, *295*, 583–592, doi:10.1016/j.epsl.2010.04.044.
Gibbs, S. J., T. J. Bralower, P. R. Bown, J. C. Zachos, and L. M. Bybell (2006a), Shelf and open-ocean calcareous phytoplankton assemblages across the Paleocene-Eocene Thermal Maximum: Implications for global productivity gradients, *Geology*, *34*(4), 233, doi:10.1130/g22381.1.
Gibbs, S. J., P. R. Bown, J. A. Sessa, T. J. Bralower, and P. A. Wilson (2006b), Nannoplankton extinction and origination across the Paleocene-Eocene Thermal Maximum, *Science*, *314*(5806), 1770–1773, doi:10.1126/science.1133902.
Gibson, T. G., L. M. Bybell, and J. P. Owens (1993), Latest Paleocene lithologic and biotic events in neritic deposits of southwestern New Jersey, *Paleoceanography*, *8*(4), 495–514, doi:10.1029/93PA01367.
Glenn, S. M., C. Jones, M. Twardowski, L. Bowers, J. Kerfoot, D. Webb, and O. Schofield (2008), Glider observations of sediment resuspension in a Middle Atlantic Bight fall transition storm, *Limnol. Oceanogr.*, *53*, 2180–2196.
Gong, D., J. T. Kohut, and S. M. Glenn (2010), Seasonal climatology of wind-driven circulation on the New Jersey Shelf, *J. Geophys. Res.*, *115*, C04006, doi:10.1029/2009JC005520.
Harris, A. D. (2010), Integrated sequence stratigraphy of the Paleocene-lowermost Eocene, New Jersey coastal plain: Implications for eustatic and paleoceanographic change, PhD thesis, 183 p., Rutgers Univ., N. J.
Harris, A. D., K. G. Miller, J. V. Browning, P. J. Sugarman, R. K. Olsson, B. S. Cramer, and J. D. Wright (2010), Integrated stratigraphic studies of Paleocene-lowermost Eocene sequences, New Jersey Coastal Plain: Evidence for glacioeustatic control, *Paleoceanography*, *25*, PA3211, doi:10.1029/2009PA001800.
Hilting, A. K., L. R. Kump, and T. J. Bralower (2008), Variations in the oceanic vertical carbon isotope gradient and their implications for the Paleocene-Eocene biological pump, *Paleoceanography*, *23*, PA3222, doi:10.1029/2007PA001458.
Hollis, C. J., B. R. Hines, K. Littler, V. Villasante-Marcos, D. K. Kulhanek, C. P. Strong, J. C. Zachos, S. M. Eggins, L. Northcote, and A. Phillips (2015), Onset of the Paleocene–Eocene Thermal Maximum in the southern Pacific Ocean (DSDP Site 277, Campbell Plateau), *Clim. Past Discuss.*, *11*, 243–278, doi:10.5194/cpd-11-243-2015.
Huber, M., and R. Caballero (2003), Eocene El Niño: Evidence for robust tropical dynamics in the "hothouse", *Science*, *299*, 877–881, doi:10.1126/science.1078766.
Huber, M., and R. Caballero (2011), The early Eocene equable climate problem revisited, *Clim. Past*, *7*, 603–633, doi:10.5194/cp-7-603-2011.
Iakovleva, A. I., H. Brinkhuis, and C. Cavagnetto (2001), Late Palaeocene-Early Eocene dinoflagellate cysts from the Turgay Strait, Kazakhstan; correlations across ancient seaways, *Palaeogeogr. Palaeoclimatol. Palaeoecol.*, *172*, 243–268.

John, C. M., S. M. Bohaty, J. C. Zachos, A. Sluijs, S. Gibbs, H. Brinkhuis, and T. J. Bralower (2008), North American continental margin records of the Paleocene-Eocene Thermal Maximum: Implications for global carbon and hydrological cycling, *Paleoceanography*, *23*, PA2217, doi:10.1029/2007PA001465.

Kahn, A., and M.-P. Aubry (2004), Provincialism associated with the Paleocene/Eocene Thermal Maximum: Temporal constraint, *Mar. Micropaleontol.*, *52*, 117–131, doi:10.1016/j.marmicro.2004.04.003.

Katz, M. E., D. K. Pak, G. R. Dickens, and K. G. Miller (1999), The source and fate of massive carbon input during the latest Paleocene Thermal Maximum, *Science*, *286*, 1531–1533.

Katz, M. E., B. S. Cramer, A. Franzese, B. Hönisch, K. G. Miller, Y. Rosenthal, and J. D. Wright (2010), Traditional and emerging geochemical proxies in foraminifera, *J. Foraminiferal Res.*, *40*(2), 165–192, doi:10.2113/gsjfr.40.2.165.

Kelly, D. C., T. J. Bralower, and J. C. Zachos (1998), Evolutionary consequences of the latest Paleocene Thermal Maximum for tropical planktonic foraminifera, *Palaeogeogr. Palaeoclimatol. Palaeoecol.*, *141*, 139–161.

Kennett, J. P., and L. D. Stott (1991), Abrupt deep-sea warming, palaeoceanographic changes and benthic extinctions at the end of the Palaeocene, *Nature*, *353*, 225–229.

Kirtland Turner, S., and A. Ridgwell (2016), Development of a novel empirical framework for interpreting geological carbon isotope excursions, with implications for the rate of carbon injection across the PETM, *Earth Planet. Sci. Lett.*, *435*, 1–13, doi:10.1016/j.epsl.2015.11.027.

Koch, P. L., J. C. Zachos, and P. D. Gingerich (1992), Correlation between isotope records in marine and continental carbon reservoirs near the Palaeocene/Eocene boundary, *Nature*, *358*, 319–322.

Kopp, R. E., D. Schumann, T. D. Raub, D. S. Powars, L. V. Godfrey, N. L. Swanson-Hysell, A. C. Maloof, and H. Vali (2009), An Appalachian Amazon? Magnetofossil evidence for the development of a tropical river-like system in the mid-Atlantic United States during the Paleocene-Eocene Thermal Maximum, *Paleoceanography*, *24*, PA4211, doi:10.1029/2009PA001783.

Lentz, S. J., and R. Limeburner (1995), The Amazon River plume during AMASSEDS: Spatial characteristics and salinity variability, *J. Geophys. Res.*, *100*(2), 2355–2375, doi:10.1029/94JC01411.

Lombardi, C. J. (2013), Lithostratigraphy and clay mineralogy of Paleocene-Eocene Thermal Maximum sediments at Wilson Lake, NJ, M.S. thesis, 94 p., Rutgers Univ., N. J.

Lu, G., and G. Keller (1996), Separating ecological assemblages using stable isotope signals: Late Paleocene to early Eocene planktonic foraminifera, DSDP Site 577, *J. Foraminiferal Res.*, *26*(2), 103–112.

Lunt, D. J., et al. (2012), A model–data comparison for a multi-model ensemble of early Eocene atmosphere-ocean simulations: EoMIP, *Clim. Past*, *8*, 1717–1736, doi:10.5194/cp-8-1717-2012.

Makarova, M., K. G. Miller, J. D. Wright, Y. Rosenthal, T. Babila, and J. V. Browning (2013), Paleoenvironmental changes associated with the PETM, Millville (ODP Leg 174AX), New Jersey coastal plain, American Geophysical Union, Fall Meeting 2013, Abstract P23B-1971.

McInerney, F. A., and S. L. Wing (2011), The Paleocene-Eocene Thermal Maximum: A perturbation of carbon cycle, climate, and biosphere with implications for the future, *Annu. Rev. Earth Planet. Sci.*, *39*, 489–516.

Menschel, E., H. E. González, and R. Giesecke (2016), Coastal-oceanic distribution gradient of coccolithophores and their role in the carbonate flux of the upwelling system off Concepción, Chile (36°S), *J. Plankton Res.*, *38*(4), 798–817, doi:10.1093/plankt/fbw037.

Miller, K. G., et al. (1998), Bass River site, in *Proceedings of the Ocean Drilling Program*, *Initial Rep.*, vol. 174AX, edited by K. G. Miller et al., pp. 5–43, Ocean Drilling Program, College Station, Tex.

Miller, K. G., et al. (1999), Ancora site, in *Proceedings of the Ocean Drilling Program*, *Initial Rep.*, vol. 174AX, edited by K. G. Miller et al., pp. 1–65, Ocean Drilling Program, College Station, Tex.

Murphy, B. H., K. A. Farley, and J. C. Zachos (2010), An extraterrestrial ^{3}He-based timescale for the Paleocene-Eocene Thermal Maximum (PETM) from Walvis Ridge, IODP Site 1266, *Geochim. Cosmochim. Acta*, *74*, 5098–5108.

Norris, R. D. (1996), Symbiosis as an evolutionary innovation in the radiation of Paleocene planktic foraminifera, *Paleobiology*, *22*, 461–480.

Olsson, R. K., C. Hemleben, W. A. Berggren, and B. T. Huber (Eds.) (1999), *Atlas of Paleocene Planktonic Foraminifera, Smithsonian Contributions to Paleobiology*, vol. 85, pp. 252, Smithsonian Institution Press, Washington, D. C.

Pagani, M., N. Pedentchouk, M. Huber, A. Sluijs, S. Schouten, H. Brinkhuis, J. S. Sinninghe Damsté, G. R. Dickens, and the Expedition 302 Scientists (2006), Arctic hydrology during global warming at the Palaeocene/Eocene Thermal Maximum, *Nature*, *442*, 671–675.

Pearson, P. N., and M. R. Palmer (1999), Middle Eocene seawater ph and atmospheric carbon dioxide concentrations, *Science*, *284*, 1824–1826, doi:10.1126/science.284.5421.1824.

Pearson, P. N., N. J. Shackleton, and M. A. Hall (1993), Stable isotope paleoecology of middle Eocene planktonic foraminifera and multispecies isotope stratigraphy, DSDP Site 523, South Atlantic, *J. Foraminiferal Res.*, *23*, 123–140.

Pearson, P. N., R. K. Olsson, B. T. Huber, C. Hemleben, and W. A. Berggren (Eds.) (2006), *Atlas of Eocene Planktonic Foraminifera, Cushman Foundation for Foraminiferal Research Special Publications*, vol. 41, pp. 513, Washington, D. C.

Pearson, P. N., P. W. Ditchfield, J. Singano, K. G. Harcourt-Brown, C. J. Nicholas, R. K. Olsson, N. J. Shackleton, and M. A. Hall (2001), Warm tropical sea surface temperatures in the Late Cretaceous and Eocene epochs, *Nature*, *413*, 481–487.

John, E. H., P. N. Pearson, H. K. Coxall, H. Birch, B. S. Wade, and G. L. Foster (2013), Warm ocean processes and carbon cycling in the Eocene, *Philos. Trans. R. Soc. A*, *371*, 1–20, doi:10.1098/rsta.2013.0099.

Penman, D. E., B. Hönisch, R. E. Zeebe, E. Thomas, and J. C. Zachos (2014), Rapid and sustained surface ocean acidification during the Paleocene-Eocene Thermal Maximum, *Paleoceanography*, *29*, 357–369, doi:10.1002/2014PA002621.

Powars, D. S., and L. E. Edwards (2015), Paleocene-Eocene Thermal Maximum lithofacies across the mid-Atlantic coastal plain: Sedimentalogical analysis of 100's of stacked turbidite packages, Abstract, 2015 GSA Annual Meeting in Baltimore, Maryland, USA (1–4 November 2015), Paper No. 247-10.

Powell, A. J., H. Brinkhuis, and J. P. Bujak (1996), Upper Paleocene-Lower Eocene dinoflagellate cyst sequence biostratigraphy of southeast England, in *Correlation of the Early Paleogene in Northwest Europe*, *Geol. Soc. Spec. Publ.*, vol. 101, edited by R. W. O. B. Knox, R. M. Corfield, and R. S. Dunay, pp. 145–183.

Quillévéré, F., R. D. Norris, I. Moussa, and W. A. Berggren (2001), Role of photosymbiosis and biogeography in the diversification of early Paleogene acarininids (planktonic foraminifera), *Paleobiology*, *27*, 311–326.

Ravelo, A. C., and R. G. Fairbanks (1992), Oxygen isotopic composition of multiple species of planktonic foraminifera: Recorders of the modern photic zone temperature gradient, *Paleoceanography*, *7*(6), 815–831, doi:10.1029/92PA02092.

Reynolds, L., and R. C. Thunell (1985), Seasonal succession of planktonic foraminifera in the subpolar North Pacific, *J. Foraminiferal Res.*, *15*(4), 282–301.

Röhl, U., T. Westerhold, T. J. Bralower, and J. C. Zachos (2007), On the duration of the Paleocene-Eocene Thermal Maximum (PETM), *Geochem. Geophys. Geosyst.*, *8*, Q12002, doi:10.1029/2007GC001784.

Self-Trail, J. M., D. S. Powars, D. K. Watkins, and G. A. Wandless (2012), Calcareous nannofossil assemblage changes across the Paleocene–Eocene Thermal Maximum: Evidence from a shelf setting, *Mar. Micropaleontol.*, *92–93*, 61–80, doi:10.1016/j.marmicro.2012.05.003.

Sexton, P. F., P. A. Wilson, and P. N. Pearson (2006), Microstructural and geochemical perspectives on planktic foraminiferal preservation: "Glassy" versus "frosty", *Geochem. Geophys. Geosyst.*, *7*, Q12P19, doi:10.1029/2006GC001291.

Sluijs, A., and H. Brinkhuis (2009), A dynamic climate and ecosystem state during the Paleocene-Eocene Thermal Maximum: Inferences from dinoflagellate cyst assemblages on the New Jersey Shelf, *Biogeosciences*, *6*, 1755–1781.

Sluijs, A., et al. (2006), Subtropical Arctic Ocean temperatures during the Palaeocene/Eocene Thermal Maximum, *Nature*, *441*, 610–613.

Sluijs, A., H. Brinkhuis, S. Schouten, S. M. Bohaty, C. M. John, J. C. Zachos, G. J. Reichart, J. S. Sinninghe Damsté, E. M. Crouch, and G. R. Dickens (2007), Environmental precursors to rapid light carbon injection at the Palaeocene/Eocene boundary, *Nature*, *450*(7173), 1218–1221, doi:10.1038/nature06400.

Sluijs, A., P. K. Bijl, S. Schouten, U. Röhl, G.-J. Reichart, and H. Brinkhuis (2011), Southern ocean warming, sea level and hydrological change during the Paleocene-Eocene Thermal Maximum, *Clim. Past*, *7*, 47–61, doi:10.5194/cp-7-47-2011.

Spindler, M. (1996), On the salinity tolerance of the planktonic foraminifera *Neogloboquadrina pachyderma* from Antarctic sea ice, *Proc. NIPR Symp. Polar Biol.*, *9*, 85–91.

Stassen, P., E. Thomas, and R. P. Speijer (2012), Integrated stratigraphy of the Paleocene-Eocene Thermal Maximum in the New Jersey Coastal Plain: Toward understanding the effects of global warming in a shelf environment, *Paleoceanography*, *27*, PA4210, doi:10.1029/2012PA002323.

Stassen, P., E. Thomas, and R. P. Speijer (2015), Paleocene–Eocene Thermal Maximum environmental change in the New Jersey Coastal Plain: Benthic foraminiferal biotic events, *Mar. Micropaleontol.*, *115*, 1–23, doi:10.1016/j.marmicro.2014.12.001.

Stoll, H. M., N. Shimizu, D. Archer, and P. Ziveri (2007), Coccolithophore productivity response to greenhouse event of the Paleocene–Eocene Thermal Maximum, *Earth Planet. Sci. Lett.*, *258*, 192–206, doi:10.1016/j.epsl.2007.03.037.

Sugarman, P. J., et al. (2005), Millville site, in *Proceedings of the Ocean Drilling Program*, *Sci. Results*, vol. 174AX (supplement), edited by K. G. Miller et al., pp. 1–95, Ocean Drilling Program, College Station, Tex.

Thomas, D. J., T. J. Bralower, and J. C. Zachos (1999), New evidence for subtropical warming during the late Paleocene Thermal Maximum: Stable isotopes from Deep Sea Drilling Project Site 527, Walvis Ridge, *Paleoceanography*, *14*(5), 561–570, doi:10.1029/1999PA900031.

Thomas, D. J., J. C. Zachos, T. M. Bralower, E. Thomas, and S. Bohaty (2002), Warming the fuel for the fire: Evidence for the thermal dissociation of methane hydrate during the Paleocene-Eocene Thermal Maximum, *Geology*, *30*(12), 1067–1070.

Thunell, R. C., W. B. Curry, and S. Honjo (1983), Seasonal variations in the flux of planktonic foraminifera: Time series sediment trap results from the Panama Basin, *Earth Planet. Sci. Lett.*, *64*, 44–55.

Tremolada, F., and T. J. Bralower (2004), Nannofossil assemblage fluctuations during the Paleocene–Eocene Thermal Maximum at Sites 213 (Indian Ocean) and 401 (North Atlantic Ocean): Palaeoceanographic implications, *Mar. Micropaleontol.*, *52*, 107–116, doi:10.1016/j.marmicro.2004.04.002.

Tripati, A. K., and H. Elderfield (2004), Abrupt hydrographic changes in the equatorial Pacific and subtropical Atlantic from foraminiferal Mg/Ca indicate greenhouse origin for the thermal maximum at the Paleocene-Eocene boundary, *Geochem. Geophys. Geosyst.*, *5*, Q02006, doi:10.1029/2003GC000631.

Wade, B. S., N. Al-Sabouni, C. Hemleben, and D. Kroon (2008), Symbiont bleaching in fossil planktonic foraminifera, *Evol. Ecol.*, *22*, 253–265, doi:10.1007/s10682-007-9176-6.

Weijers, J. W. H., S. Schouten, A. Sluijs, H. Brinkhuis, and J. S. Sinninghe Damsté (2007), Warm arctic continents during the Palaeocene–Eocene Thermal Maximum, *Earth Planet. Sci. Lett.*, *261*, 230–238, doi:10.1016/j.epsl.2007.06.033.

Wing, S. L., G. J. Harrington, F. A. Smith, J. I. Bloch, D. M. Boyer, and K. H. Freeman (2005), Transient floral change and rapid global warming at the Paleocene-Eocene boundary, *Science*, *310*, 993–996.

Wright, J. D., and M. F. Schaller (2013), Evidence for a rapid release of carbon at the Paleocene-Eocene Thermal Maximum, *Proc. Natl. Acad. Sci. U.S.A.*, *110*(40), 15,908–15,913.

Zachos, J. C., M. W. Wara, S. M. Bohaty, M. L. Delaney, M. Rose-Petrizzo, A. Brill, T. J. Bralower, and I. Premoli-Silva (2003), A transient rise in tropical sea surface temperature during the Paleocene-Eocene Thermal Maximum, *Science*, *302*, 1551–1554.

Zachos, J. C., et al. (2005), Rapid acidification of the ocean during the Paleocene-Eocene Thermal Maximum, *Science*, *308*, 1611–1615, doi:10.1126/science.1109004.

Zachos, J. C., S. Schouten, S. Bohaty, T. Quattlebaum, A. Sluijs, H. Brinkhuis, S. J. Gibbs, and T. J. Bralower (2006), Extreme warming of mid-latitude coastal ocean during the Paleocene-Eocene Thermal Maximum: Inferences from TEX_{86} and isotope data, *Geology*, *34*(9), 737–740.

Zachos, J. C., S. M. Bohaty, C. M. John, H. McCarren, D. C. Kelly, and T. Nielsen (2007), The Palaeocene–Eocene carbon isotope excursion: Constraints from individual shell planktonic foraminifer records, *Philos. Trans. R. Soc. A*, *365*, 1829–1842, doi:10.1098/rsta.2007.2045.

Zapecza, O. S. (1984), Hydrogeologic framework of the New Jersey coastal plain, *U.S. Geol. Surv. Open File Rep.*, *84*(730), 1–61.

Zeebe, R. E., A. Ridgwell, and J. C. Zachos (2016), Anthropogenic carbon release rate unprecedented during the past 66 million years, *Nat. Geosci.*, *9*, 325–329, doi:10.1038/ngeo2681.